Northwest Atlantic Fisheries Organization

Advances in the Assessment of Habitat Fragmentation and Protection in the NAFO Regulatory Area

By

S. Wang[1], E. Kenchington[1], F.J. Murillo[1], C. Lirette[1], M. Koen-Alonso[2], A. Kenny[3], M. Sacau[4]

[1]Department of Fisheries and Oceans, Dartmouth, Nova Scotia, Canada.

[2]Department of Fisheries and Oceans, St. John's, Newfoundland and Labrador, Canada

[3]CEFAS, Lowestoft , Suffolk, United Kingdom.

[4]Institute of Spanish Oceanography, Vigo, Spain.

Abstract

NAFO has used kernel density analyses to identify VMEs dominated by large-sized sponges, sea pens, small and large gorgonian corals, erect bryozoans, sea squirts (*Boltenia ovifera*), and black corals. That analysis generates polygons of significant concentrations of biomass for each VME indicator which are spread across the spatial domain of the NAFO fishing footprint. There is potential for bottom contact fishing to induce changes in both the amount and configuration of habitat (e.g., decreased polygon size, increased polygon isolation, and increased edge area) through direct and indirect impacts, and it is unknown to what degree such changes may already have taken place given the long fishing history of the area. In the Report of the 13th Meeting of the NAFO Scientific Council Working Group on Ecosystem Science and Assessment (WGE-ESA), preliminary work on assessing and monitoring habitat fragmentation was presented. Here we continue that work by recalculating the indices after removing connections that are not identified through particle tracking models. We have reanalyzed the nearest neighbour distances and PX, a proximity index, for the VME polygons noted above, and for the new closed areas that will come into effect 1 January 2022. We show that PX when applied to the new closures appears sensitive to their spatial configuration which bodes will for the ability of this index to identify habitat fragmentation in the future, brought about through fishing activities and/or natural disturbances.

Introduction

NAFO has used kernel density analyses to identify VMEs dominated by large-sized sponges, sea pens, small and large gorgonian corals, erect bryozoans, sea squirts (*Boltenia ovifera*), and black corals. That analysis (Kenchington et al. 2014) generates polygons of significant concentrations of biomass for each VME indicator which are spread across the spatial domain of the NAFO fishing footprint. There is potential for bottom contact fishing to induce changes in both the amount and configuration of habitat (e.g., decreased polygon size, increased polygon isolation, and increased edge area) through direct and indirect impacts, and it is unknown to what degree such changes may already have taken place given the long fishing history of the area. Habitat fragmentation is defined as the division of habitat into smaller and more isolated fragments (Haddad et al. 2015), and can arise through both natural and anthropogenic activities (Haddad et al. 2015, Wilson et al. 2016). In the Report of the 13th Meeting of the NAFO Scientific Council Working Group on Ecosystem Science and Assessment (WGE-ESA), preliminary work on assessing and monitoring habitat fragmentation was presented (NAFO 2020).
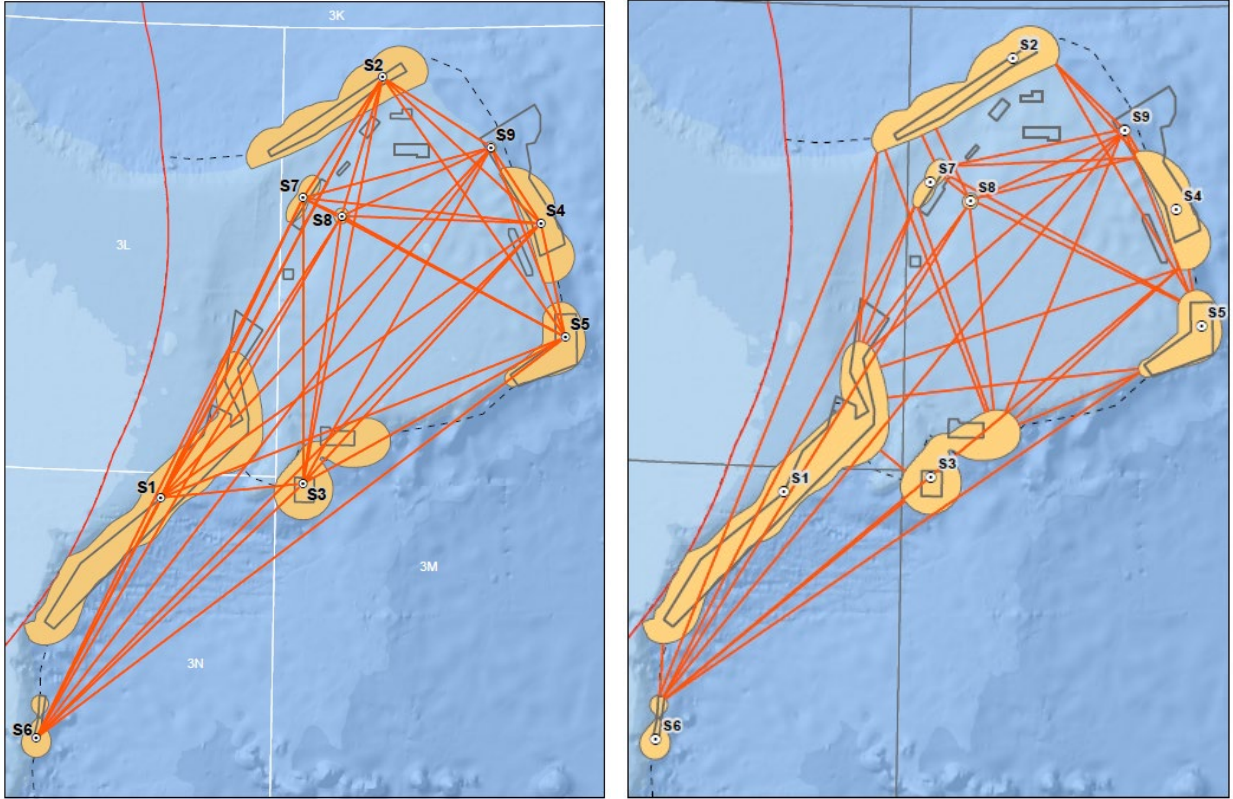
Figure 1. Nearest neighbour distance lines between large-sized sponge VME polygons in the NRA calculated from centroid to centroid (Left panel) and from the nearest edge (Right panel). NAFO closed areas for the protection of corals and sponges are indicated in grey. [from NAFO, 2020]. Dashed line represents the fishing footprint (~2000 m); red line indicates EEZ of Canada; white or grey lines represent NAFO divisions. Projection: NAD83 UTM 23.

Two methods were used to calculate nearest neighbour distances between VME polygons (NAFO, 2020): centroid to centroid, and edge to edge (Figure 1, Table 1). In addition, the average nearest neighbour ratio and a proximity index (PX) as described by Gustafson and Parker (1994), were calculated. The former can only be applied to symmetrical distributions (across all closed areas for example) while the later can only be applied to the edge-edge distances. The distance matrices used in those assessments included connections between VME polygons and between Closed Areas that may not occur (e.g., Figure 1, Table 1). Removal of connections that are unlikely to occur due to the prevailing oceanographic currents, and recalculation of the indices was proposed for the next phase of development of these indices. This needed to be done both for the VME polygons and the new Closed Areas. Here we present those results.

Table 1. Nearest neighbour distances (km) calculated from centroid to centroid (below diagonal, shaded) and from nearest edges (above diagonal) for the sponge VME polygons in the NAFO Regulatory Area (numbered as in Figure 1). The mean nearest-neighbour distance for each polygon, as a measure of relative isolation, is shown below the rows for the centroid to centroid distances and to the right of columns for the nearest edges distances. Polygons are numbered according to decreasing area. [from NAFO 2020]. Projection: NAD83 UTM 23.

	Polygon Area km²	S1	S2	S3	S4	S5	S6	S7	S8	S9	Mean Nearest-Neighbour Distance (Edge-Edge)
S1	9687.0	---	148	25	244	197	40	113	131	256	144
S2	4596.9	382	---	219	93	205	455	22	56	69	158
S3	3695.9	115	333	---	172	102	242	168	157	234	165
S4	2571.5	377	173	283	---	17	521	144	125	14	166
S5	2255.1	350	256	242	94	---	448	206	175	131	185
S6	711.9	217	600	296	579	534	---	429	448	565	394
S7	516.2	267	116	230	192	239	484	---	21	136	155
S8	119.8	269	116	217	160	205	486	34	---	122	154
S9	63.5	387	104	310	73	164	599	157	132	---	191
Mean Nearest-Neighbour Distance (Centroid-Centroid)		296	260	253	241	261	474	215	202	241	

Methods and Results

Connectivity Assessments

Lagrangian particle tracking (LPT) models are considered an important tool for assessing structural connectivity in the deep sea (e.g., Xu et al., 2018; Bracco et al., 2019; Kenchington et al., 2019; Zeng et al., 2019, Wang et al., 2020; Wang et al., 2021) and can provide strong support for the evaluation of species distribution models (Kenchington et al., 2019; Wang et al., 2021). In LPT models, virtual particles are advected by the flow fields from numerical ocean models (Lange and van Sebille, 2017). Virtual behavior, if known, can also be added to the particles so that they can act as active drifters, i.e., swimming larvae, and enable predictions of functional connectivity (sensu Tischendorf and Fahrig, 2000). Here, the Parcels framework version 2.2.2 (Lange and van Sebille, 2017; Delandmeter and van Sebille, 2019) was used to perform three-dimensional (3-D) passive particle tracking experiments in the NAFO Regulatory Area of the northwest Atlantic. The Bedford Institute of Oceanography North Atlantic Model (BNAM) (Wang et al., 2018, 2019) was used to generate the current velocity data used in the particle tracking models (Wang et al., 2020). Climatological monthly-averaged currents were obtained from the BNAM ocean model over the 1990-2015 period. A horizontal diffusivity constant, Kh = 100 m s⁻¹ was applied (Wang et al. 2020) to compensate in part for the variation lost in averaging. The proportion of particles passing over or terminating in another sponge VME polygon (Goldsmit et al., 2019) was presented as a connectivity matrix among sponge VME polygons for each model run. We use the terminology "source" to indicated the VME polygon or closure where the particles were seeded, and "sink" to indicated the polygon or closure that they travelled to as the flow is unidirectional.

Large-sized Sponge VMEs

Particles for the LPT modeling were seeded uniformly inside the sponge VME polygons (Figure 1) as in Figure 2. Rectangles encapsulating each of the nine sponge VME polygons (Figure 1) were constructed (Figure 2A) and a 1-km grid was overlain in each (Figure 2B). The projection NAD83 UTM 23 was used to construct all grids. The grid points falling within the sponge VME polygon were retained and used to seed particles for the

LPT analyses (Figure 2B). A minimum of 50 particles per area was established and additional particles were randomly placed in small sponge VME polygons.
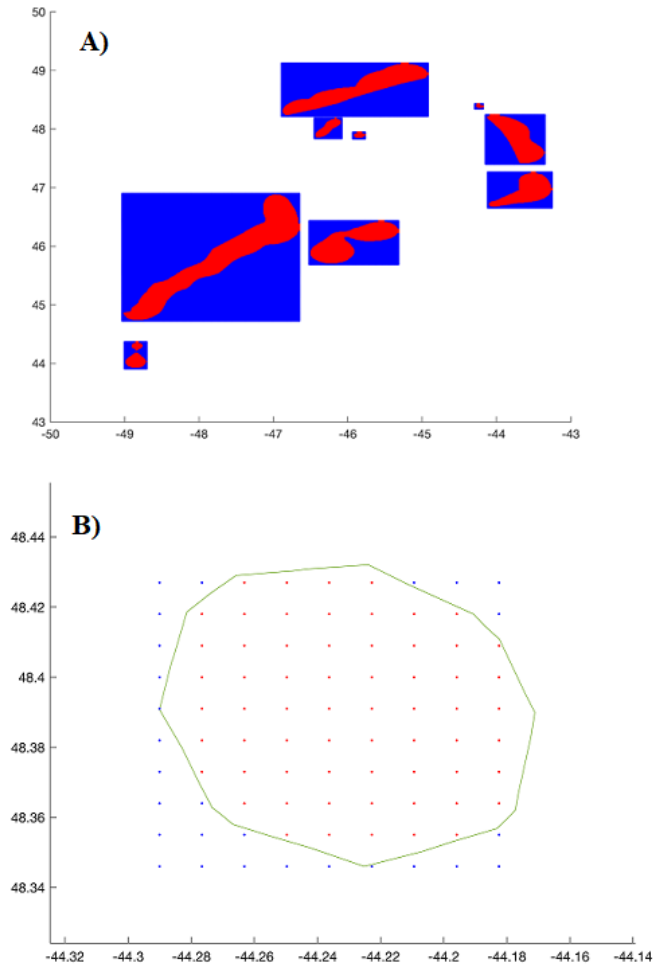

Figure 2.   Steps showing the construction of grid cells for the particle seeding for the LPT analyses among large-size sponge VMEs. A) rectangles (red and blue) were placed over each sponge VME polygon (red) within which B) a uniform grid with 1-km spacing was overlain and grid points falling within the sponge VME polygons were used to position particles to seed the analyses. Projection: NAD83 UTM 23.
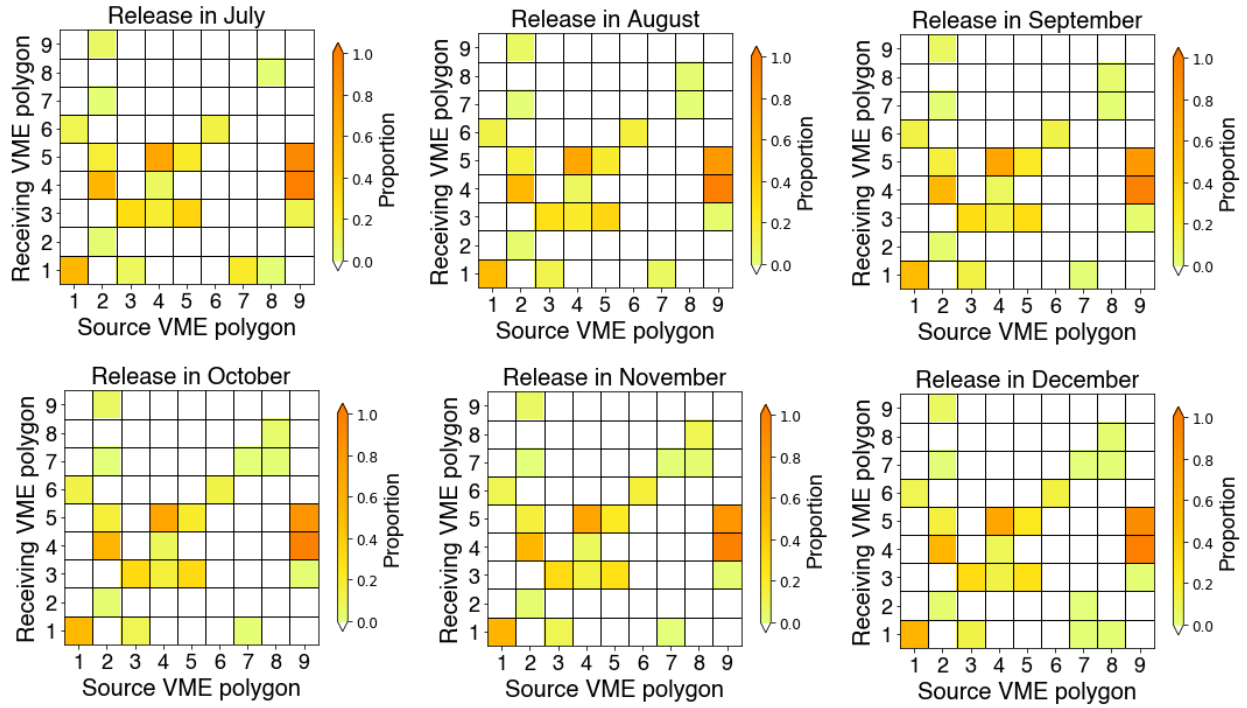
Figure 3. Connectivity matrices between sponge VME polygons for particles released for two weeks in each month from July to December (Summer and Fall) as evaluated in Wang et al. (2020). The diagonal represents particle retention. Polygon numbers are shown in Figure 1.
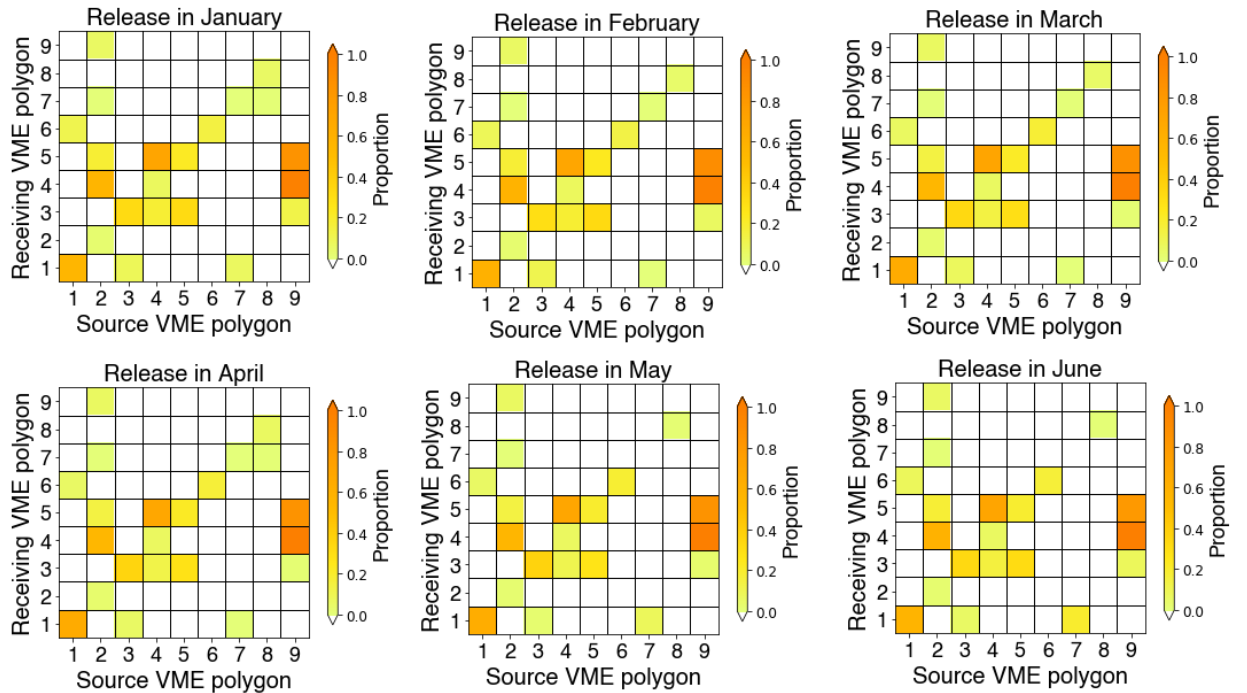

Figure 4. Connectivity matrices between sponge VME polygons for particles released for two weeks in each month from January to June (Winter and Spring). The diagonal represents particle retention. Polygon numbers are shown in Figure 1.

Wang et al. (2020) used Summer and Fall to release particles, as these are the most likely spawning season for the sponges (Kenchington et al., 2019). Here, monthly averaged currents were extracted from BNAM for each season (Winter, Spring, Summer, Fall) to confirm that no new connections were made at other times. Particles were released from the sea bed and allowed to advect for two weeks, a maximal estimate for pelagic larval duration (PLD) for all sponges (Kenchington et al., 2019). The connectivity matrices for each month are shown in Figures 3 and 4. No additional connections were made in the Winter and Spring (over Summer and Fall) as observed by Wang et al. (2020).

The nearest-neighbour distances in kilometres, calculated from centroid to centroid (Table 2) and from edge to edge (Table 3) for polygons that have a strong likelihood of connecting with one another, as indicated by the LPT analyses are provided. As connections are only unidirectional the results are presented as a square matrix. Only 16 of the 72 possible connections (excluding retentions in the same areas as the release polygons) were considered likely. Mean nearest-neighbour distances ranged from 0-242 km (centroid to centroid) and 0-126 km (edge to edge). The Proximity Index, PX, was smaller than when all connections were considered (Table 4) being 1111.8 previously (NAFO, 2020). Polygons S2 and S9 have the largest number of connections to other sponge VME polygons (Figures 3, 4).

Table 2. Unidirectional (source to sink) nearest neighbour distances (km) calculated from centroid to centroid for the sponge VME polygons in the NAFO Regulatory Area (numbered as in Figure 1) which showed connectivity (Figures 3, 4, 5). The mean nearest-neighbour distance for each polygon is shown.

			Source Sponge VME Polygon								
		Polygon Area km²	S1	S2	S3	S4	S5	S6	S7	S8	S9
Sink Sponge VME Polygon	S1	9687.0	---		115				267	269	
	S2	4596.9		---					116		
	S3	3695.9			---	283	242				310
	S4	2571.5		173		---					73
	S5	2255.1		256		94	---				164
	S6	711.9	217					---			
	S7	516.2		116					---	34	
	S8	119.8								---	
	S9	63.5		104							---
	Mean Nearest-Neighbour Distance (Centroid-Centroid)		217	162	115	188	242	0	192	152	182

Table 3. Unidirectional (source to sink) nearest neighbour distances (km) calculated from edge to edge for the sponge VME polygons in the NAFO Regulatory Area (numbered as in Figure 1) which showed connectivity (Figures 3, 4, 5). The mean nearest-neighbour distance for each polygon is shown.

|			Source Sponge VME Polygon								
		Polygon Area km²	**S1**	**S2**	**S3**	**S4**	**S5**	**S6**	**S7**	**S8**	**S9**
Sink Sponge VME Polygon	**S1**	9687.0	---		25				113	131	
	S2	4596.9		---					22		
	S3	3695.9			---	172	102				234
	S4	2571.5		93		---					14
	S5	2255.1		205		17	---				131
	S6	711.9	40					---			
	S7	516.2		22					---	21	
	S8	119.8								---	
	S9	63.5		69							---
	Mean Nearest-Neighbour Distance (Edge to Edge)		40	97	25	95	102	0	68	76	126
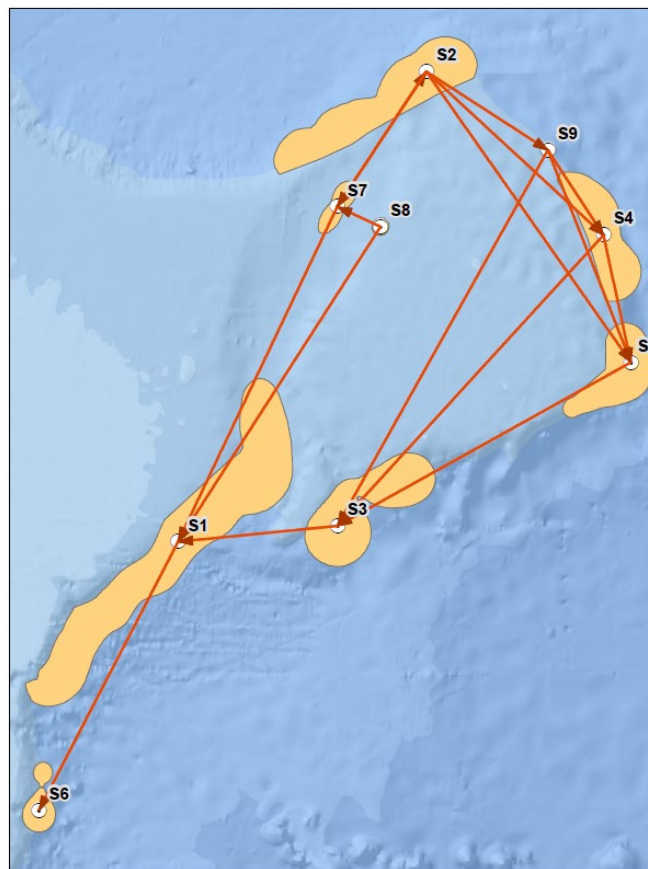
Figure 5. Unidirectional (source to sink) connectivity for the sponge VME polygons in the NAFO Regulatory Area (numbered as in Figure 1) which showed connectivity (Figures 3, 4).

Table 4.   Isolation/Proximity indices for the large-sized sponge VME polygons in the NAFO Regulatory Area calculated using only the connections that were shown to be possible through the LPT modeling (Figures 3 4 and 5).

Distance Measurement Method	Mean Nearest-Neighbour Distance Over All Polygons Pairs	Proximity Index (PX)
Centroid-Centroid	161	
Edge-Edge	70	806.04

Sea Pen VMEs

Particles for the LPT modeling were seeded uniformly inside the sea pen VME polygons (Figure 6) as in Figure 7. Rectangles encapsulating each of the eleven sea pen VME polygons were constructed (Figure 7A) and a 1-km grid was overlain in each (Figure 7B). The projection NAD83 UTM 23 was used to construct all grids. The grid points falling within the sea pen VME polygon were retained and used to seed particles for the LPT analyses (Figure 7B). A minimum of 50 particles per area was established and additional particles were randomly placed in small sea pen VME polygons.
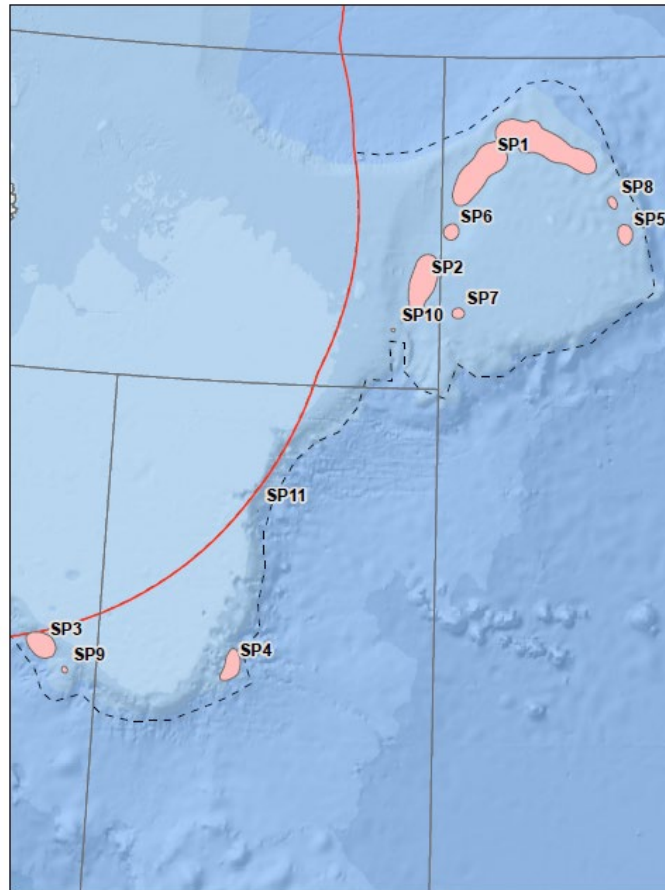

Figure 6.   Location of the Sea Pen (SP) VMEs numbered according to VME area with SP1 having the largest area (Table 6). VME polygons were produced following Kenchington et al. (2019). Dashed line represents the fishing footprint (~2000 m); red line indicates EEZ of Canada. NAD83 UTM 23 projection.
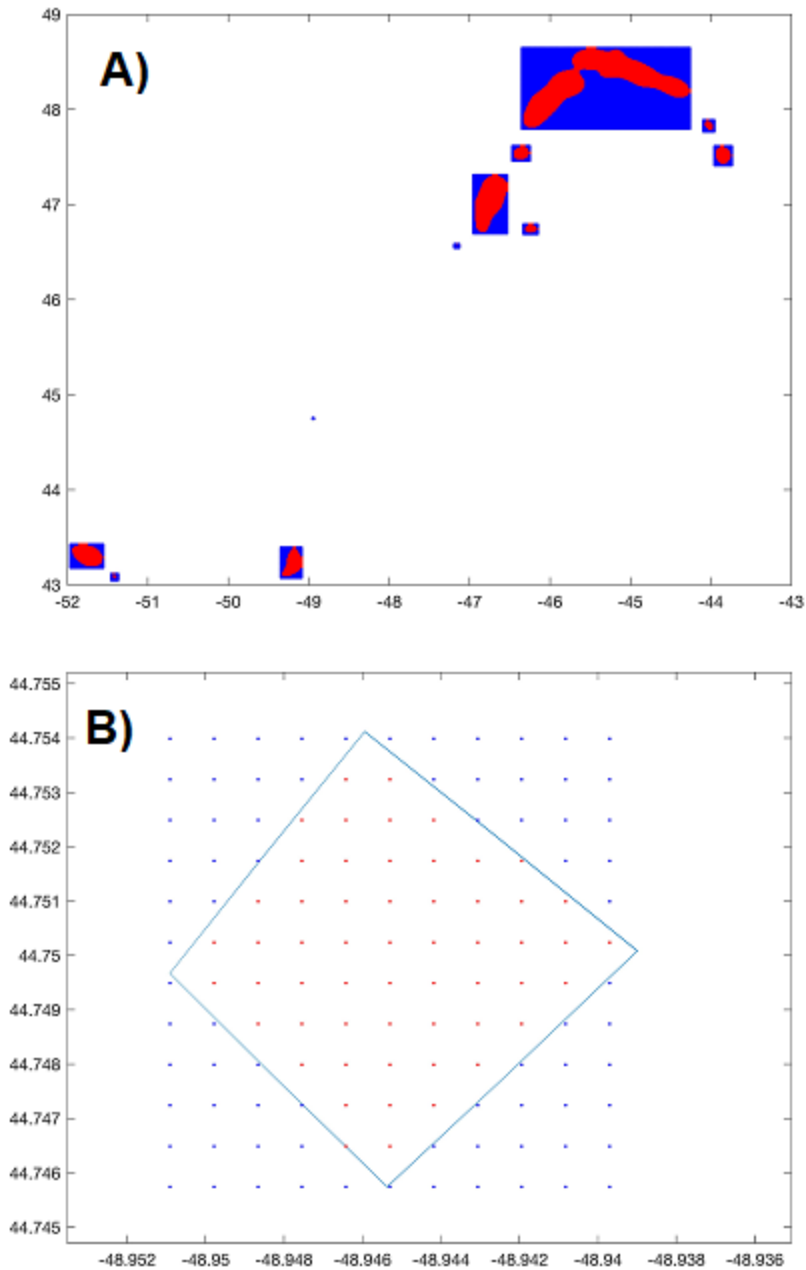
Figure 7. Steps showing the construction of grid cells for the particle seeding for the LPT analyses among sea pen VMEs. A) rectangles (red and blue) were placed over each sea pen VME polygon (red) within which B) a uniform grid with 1-km spacing was overlain and grid points falling within the sea pen VME polygons (red) were used to position particles to seed the analyses. Projection: NAD83 UTM 23.
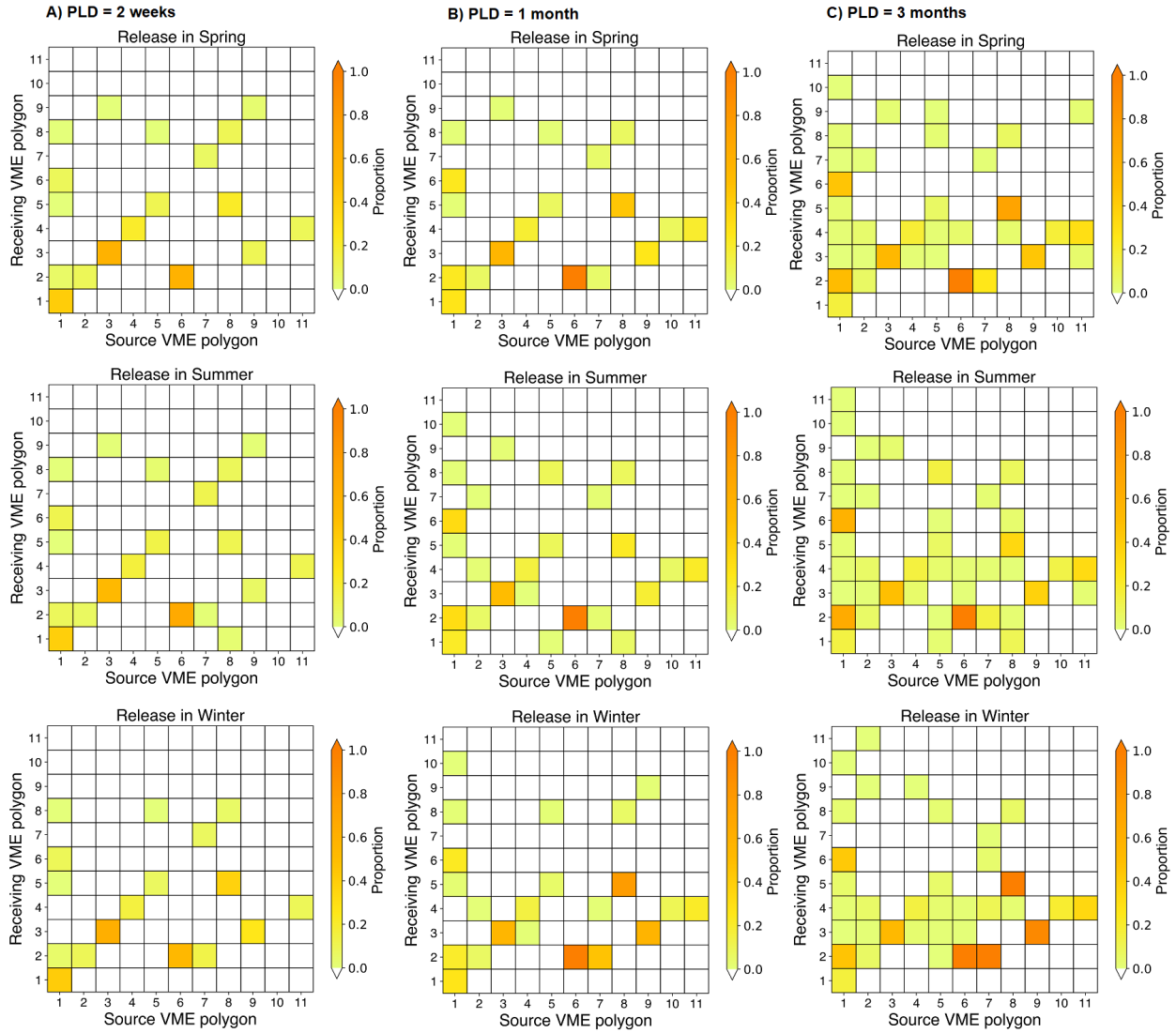
Figure 8. Connectivity matrices between the eleven sea pen VME polygons for particles released for two weeks, one month and three months (PLD) in the Spring, Summer and Winter as evaluated in Wang et al. (2020). The diagonal represents particle retention. Polygon numbers are shown in Figure 6.

**Table 5.** Unidirectional (source to sink) nearest neighbour distances (km) calculated from centroid to centroid for the sea pen VME polygons in the NAFO Regulatory Area (numbered as in Figure 6) which showed connectivity (Figure 8). The mean nearest-neighbour distance for each polygon is shown.

		Polygon Area km²	Source Sea Pen VME Polygon										
			SP1	SP2	SP3	SP4	SP5	SP6	SP7	SP8	SP9	SP10	SP11
Sink Sea Pen VME Polygon	SP1	5030.1	---				169			143			
	SP2	1492.8	152	---			226	64	51	224			
	SP3	685.8	716	571	---	208	775	632			37		276
	SP4	506.7	616	465		---	635	529	456	652		405	171
	SP5	283.8	169				---			37			
	SP6	228.4	88				189	---	89	178			
	SP7	124.4	170	51					---				
	SP8	97.3	143				37			---			
	SP9	34.3		572	37	181	771				---		272
	SP10	13.6	212									---	
	SP11	0.4	456	305									---
	Mean Nearest-Neighbour Distance (Centroid-Centroid)		302	393	37	195	400	408	199	247	37	405	240

Table 6. Unidirectional (source to sink) nearest neighbour distances (km) calculated from edge to edge for the sea pen VME polygons in the NAFO Regulatory Area (numbered as in Figure 6) which showed connectivity (Figure 8). The mean nearest-neighbour distance for each polygon is shown.

		Polygon Area km²	Source Sea Pen VME Polygon										
			SP1	SP2	SP3	SP4	SP5	SP6	SP7	SP8	SP9	SP10	SP11
Sink Sea Pen VME Polygon	SP1	5030.1	---				65			32			
	SP2	1492.8	61	---			197	24	29	196			
	SP3	685.8	644	525	---	181	753	610			16		262
	SP4	506.7	539	410		---	608	502	432	630		385	151
	SP5	283.8	65				---			19			
	SP6	228.4	20				173	---	74	165			
	SP7	124.4	111	29					---				
	SP8	97.3	32				19			---			
	SP9	34.3		536	16	165	759				---		268
	SP10	13.6	150									---	
	SP11	0.4	396	270									---
	Mean Nearest-Neighbour Distance (Edge-Edge)		224	354	16	173	368	379	178	208	16	385	227

Wang et al. (2020) used Spring, Summer and Winter to release particles, as these are the most likely spawning season for the sea pens (Kenchington et al., 2019). Here, monthly averaged currents were extracted from BNAM

for each season (Winter, Spring, Summer) and particles were released from the sea bed and allowed to advect for two weeks, one month and three months, the latter a maximal estimate for pelagic larval duration (PLD) for sea pens (Kenchington et al., 2019). The connectivity matrices for each season are shown in Figure 8.

The nearest-neighbour distances in kilometres, calculated from centroid to centroid (Table 5) and from edge to edge (Table 6) for sea pen polygons that have a strong likelihood of connecting with one another, as indicated by the LPT analyses are provided. As connections are only unidirectional from source to sink, the results are presented as a square matrix. Only 40 of the 110 possible connections (excluding retentions) were considered likely. Mean nearest-neighbour distances ranged from 37-408 km (centroid to centroid) and 16-385 km (edge to edge). The Proximity Index, PX, was slightly smaller than when all connections were considered (Table 7) being 394.2 previously (NAFO, 2020). All sea pen VME polygons are connected to at least one other VME polygon (Figure 8). The largest polygon SP1 has the most connections but SP2, SP5 and SP8 connect to 5 or more other polygons (Figure 8).

Table 7. Isolation/Proximity indices for the sea pen VME polygons in the NAFO Regulatory Area calculated using only the connections that were shown to be possible through the LPT modeling (Figure 8).

Distance Measurement Method	Mean Nearest-Neighbour Distance Over All Polygons Pairs	Proximity Index (PX)
Centroid-Centroid	303	
Edge-Edge	263	385.0

Large Gorgonian Corals

Particles for the LPT modeling were seeded uniformly inside the large gorgonian coral VME polygons (Figure 9) as in Figure 10. Rectangles encapsulating each of the twelve large gorgonian coral VME polygons were constructed (Figure 10A) and a 1-km grid was overlain in each (Figure 10B). The projection NAD83 UTM 23 was used to construct all grids. The grid points falling within the twelve large gorgonian coral VME polygons were retained and used to seed particles for the LPT analyses (Figure 10B). A minimum of 50 particles per area was established and additional particles were randomly placed in small-sized large gorgonian coral VME polygons.

Wang et al. (2020) used averaged currents over the BNAM time frame (1990-2015) to release particles, as the spawning season for the large gorgonian corals in the region is unknown (Kenchington et al., 2019). Particles were released from the sea bed and allowed to advect for two weeks, one month and three months, the latter a maximal estimate for pelagic larval duration (PLD) for the large gorgonian corals in this area (Kenchington et al., 2019). The connectivity matrices for PLD are shown in Figure 11. Only polygons showing connections were retained.

The nearest-neighbour distances in kilometres, calculated from centroid to centroid (Table 8) and from edge to edge (Table 9) for large gorgonian coral polygons that have a strong likelihood of connecting with one another, as indicated by the LPT analyses are provided. As connections are only unidirectional from source to sink, the results are presented as a square matrix. Only 20 of the 132 possible connections (excluding retentions) were considered likely. Mean nearest-neighbour distances ranged from 0-410 km (centroid to centroid) and 0-383 km (edge to edge). The Proximity Index, PX, was smaller than when all connections were considered (Table 10) being 255.1 previously (NAFO, 2020). Polygons LGC4, LGC5, LGC9 and LGC11 do not connect to other polygons, the first because of its position downstream from the other polygons (Figures 9, 11).
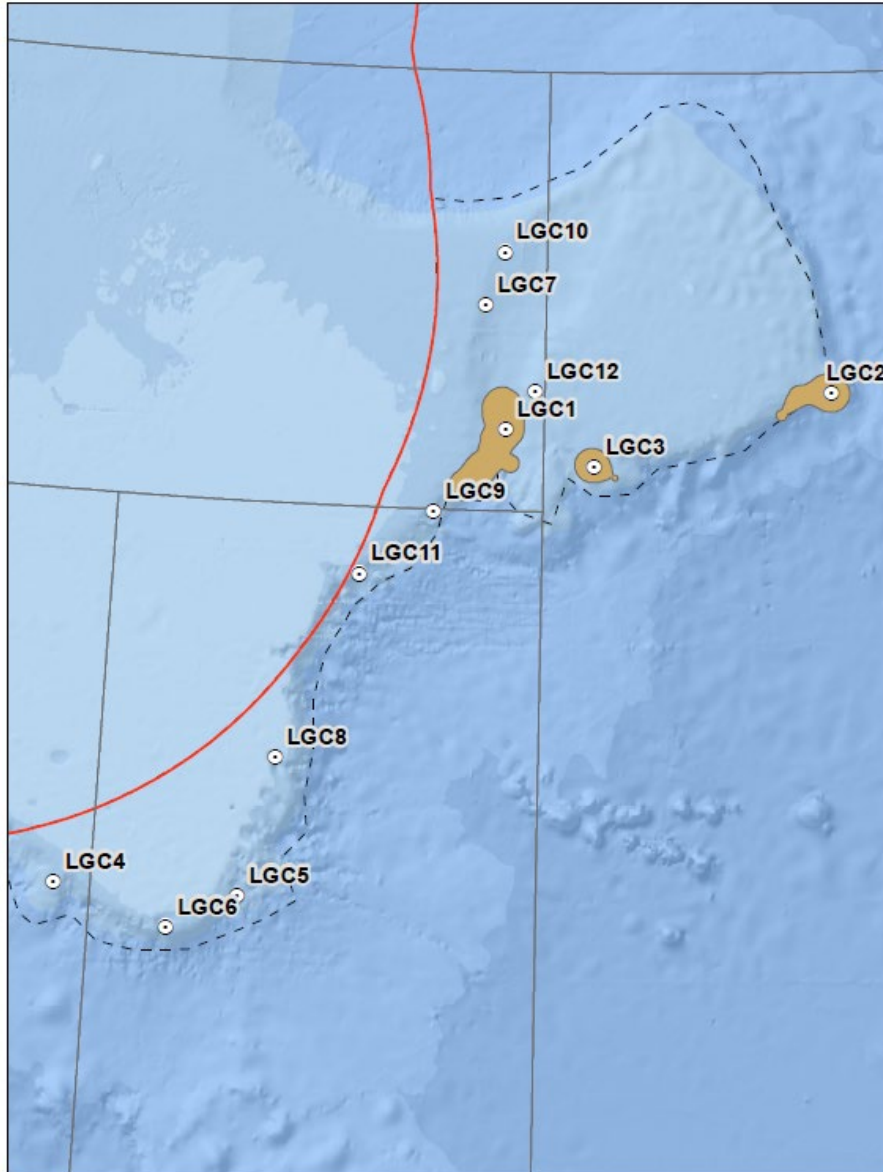
Figure 9. Location of the large gorgonian coral (LGC) VMEs numbered according to VME area with LGC1 having the largest area (Table 8). VME polygons were produced following Kenchington et al. (2019). Dashed line represents the fishing footprint (~2000 m); red line indicates EEZ of Canada. NAD83 UTM 23 projection.
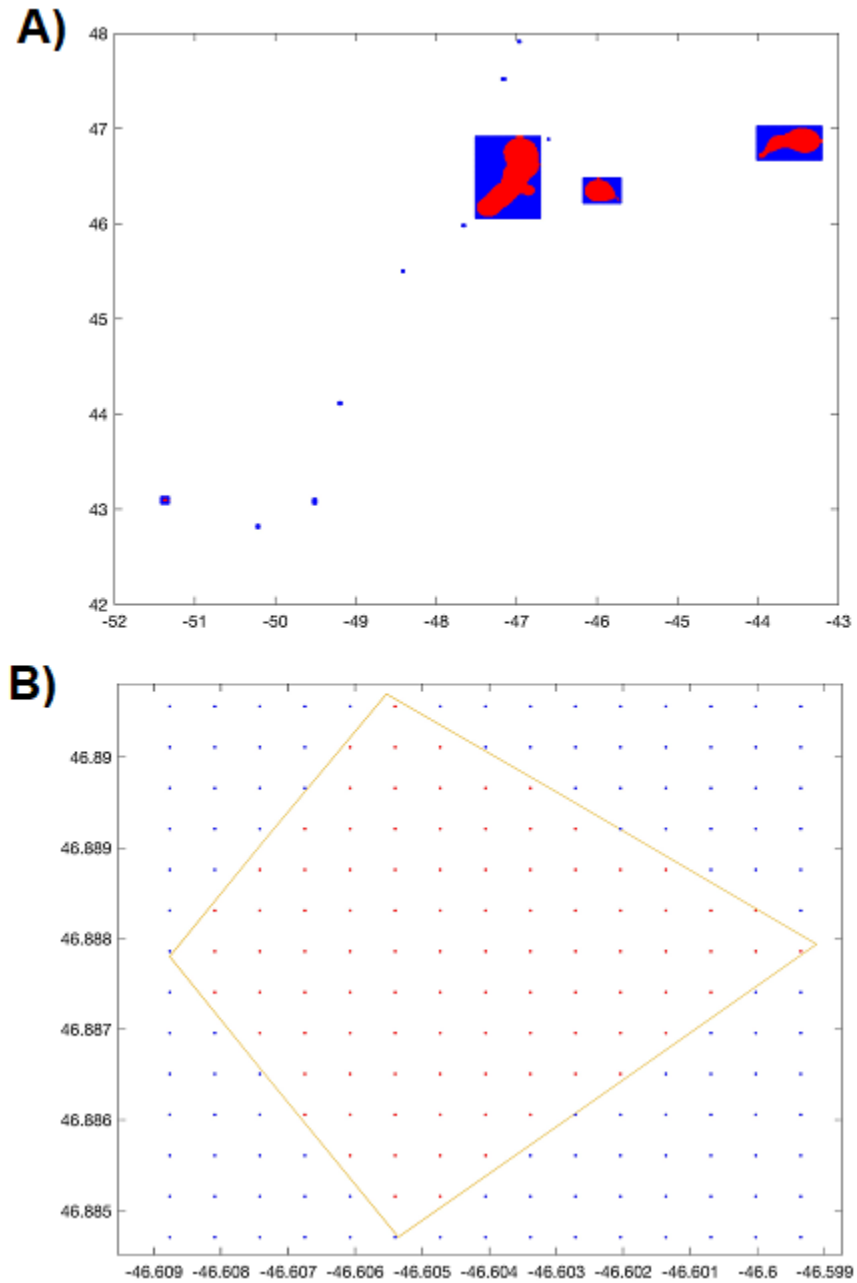
Figure 10. Steps showing the construction of grid cells for the particle seeding for the LPT analyses among large gorgonian coral VMEs. A) rectangles (red and blue) were placed over each large gorgonian coral VME polygon (red) within which B) a uniform grid with 1-km spacing was overlain and grid points falling within the large gorgonian coral VME polygons (red) were used to position particles to seed the analyses. Projection: NAD83 UTM 23.
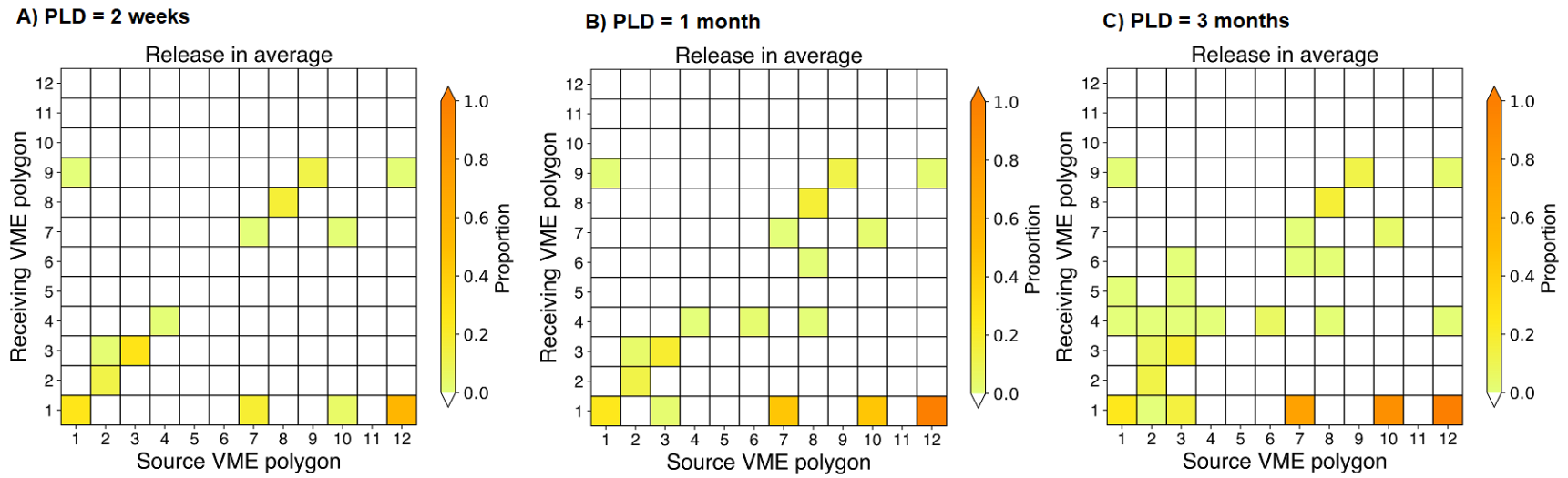
Figure 11. Connectivity matrices between the twelve large gorgonian VME polygons for particles released for two weeks, one month and three months (PLD) using monthly-averaged currents as evaluated in Wang et al. (2020). The diagonal represents particle retention. Polygon numbers are shown in Figure 9.

Table 8. Unidirectional (source to sink) nearest neighbour distances (km) calculated from centroid to centroid for the large gorgonian coral VME polygons in the NAFO Regulatory Area (numbered as in Figure 9) which showed connectivity (Figure 11). The mean nearest-neighbour distance for each polygon is shown.

|			Source Large Gorgonian Coral VME Polygon											
		Polygon Area km²	LGC1	LGC2	LGC3	LGC4	LGC5	LGC6	LGC7	LGC8	LGC9	LGC10	LGC11	LGC12
Sink Large Gorgonian Coral VME Polygon	LGC1	2964.3	---	270	79				104			146		39
	LGC2	1274.9		---										
	LGC3	703.8		204	---									
	LGC4	41.6	526	755	560	---		99		209				565
	LGC5	9.9	442		458		---							
	LGC6	3.1			517			---	575	166				
	LGC7	3.0							---			46		
	LGC8	2.3								---				
	LGC9	1.4	90								---			129
	LGC10	1.2										---		
	LGC11	0.8											---	
	LGC12	0.2												---
	Mean Nearest-Neighbour Distance (Centroid-Centroid)		353	410	404	0	0	99	340	188	0	96	0	244

Table 9. Unidirectional (source to sink) nearest neighbour distances (km) calculated from edge to edge for the large gorgonian coral VME polygons in the NAFO Regulatory Area (numbered as in Figure 9) which showed connectivity (Figure 11). The mean nearest-neighbour distance for each polygon is shown.

		Polygon Area km²	Source Large Gorgonian Coral VME Polygon											
			LGC1	LGC2	LGC3	LGC4	LGC5	LGC6	LGC7	LGC8	LGC9	LGC10	LGC11	LGC12
Sink Large Gorgonian Coral VME Polygon	LGC1	2964.3	---	207	46				68			110		13
	LGC2	1274.9		---										
	LGC3	703.8		139	---									
	LGC4	41.6	452	703	542	---		94		204				561
	LGC5	9.9	369		441		---							
	LGC6	3.1			501			---	573	164				
	LGC7	3.0							---			45		
	LGC8	2.3								---				
	LGC9	1.4	19								---			128
	LGC10	1.2										---		
	LGC11	0.8											---	
	LGC12	0.2												---
	Mean Nearest-Neighbour Distance (Edge-Edge)		280	350	383	0	0	94	321	184	0	78	0	234

Table 10. Isolation/Proximity indices for the large gorgonian coral VME polygons in the NAFO Regulatory Area calculated using only the connections that were shown to be possible through the LPT modelling (Figure 11).

Distance Measurement Method	Mean Nearest-Neighbour Distance Over All Polygons Pairs	Proximity Index (PX)
Centroid-Centroid	299	
Edge-Edge	269	180.6

Small Gorgonian Corals

Particles for the LPT modeling were seeded uniformly inside the small gorgonian coral VME polygons (Figure 12) as in Figure 13. Rectangles encapsulating each of the nine small gorgonian coral VME polygons were constructed (Figure 13A) and a 1-km grid was overlain in each (Figure 13B). The projection NAD83 UTM 23 was used to construct all grids. The grid points falling within the small gorgonian coral VME polygons were retained and used to seed particles for the LPT analyses (Figure 13B). A minimum of 50 particles per area was established and additional particles were randomly placed in small-sized small gorgonian coral VME polygons.

Wang et al. (2020) used averaged currents over the BNAM time frame (1990-2015) to release particles, as the spawning season for the small gorgonian corals in the region is unknown (Kenchington et al., 2019). Particles were released from the sea bed and allowed to advect for two weeks, one month and three months, the latter a maximal estimate for pelagic larval duration (PLD) for the large gorgonian corals in this area (Kenchington et al., 2019). The connectivity matrices for PLD are shown in Figure 14. Only polygons showing connections were retained.

The nearest-neighbour distances in kilometres, calculated from centroid to centroid (Table 11) and from edge to edge (Table 12) for small gorgonian coral polygons that have a strong likelihood of connecting with one another, as indicated by the LPT analyses are provided. As connections are only unidirectional from source to sink, the results are presented as a square matrix. Only 24 of the 72 possible connections (excluding retentions) were considered likely. Mean nearest-neighbour distances ranged from 0-590 km (centroid to centroid) and 0-571 km (edge to edge). The Proximity Index, PX, was much smaller than when all connections were considered (Table 13) being 125.2 previously (NAFO, 2020). This is due to the largest area, SGC1, having no connections due to its downstream position relative to the other VMEs.

SGC2 emerges as very important for connectivity to other VME polygons if PLD is 3 months. SGC1, the largest area is downstream of the other areas and so does not appear as an important seed source. SGC5, SGC6 and SGC8 show connectivity to two or more polygons under all PLD (Figure 14).
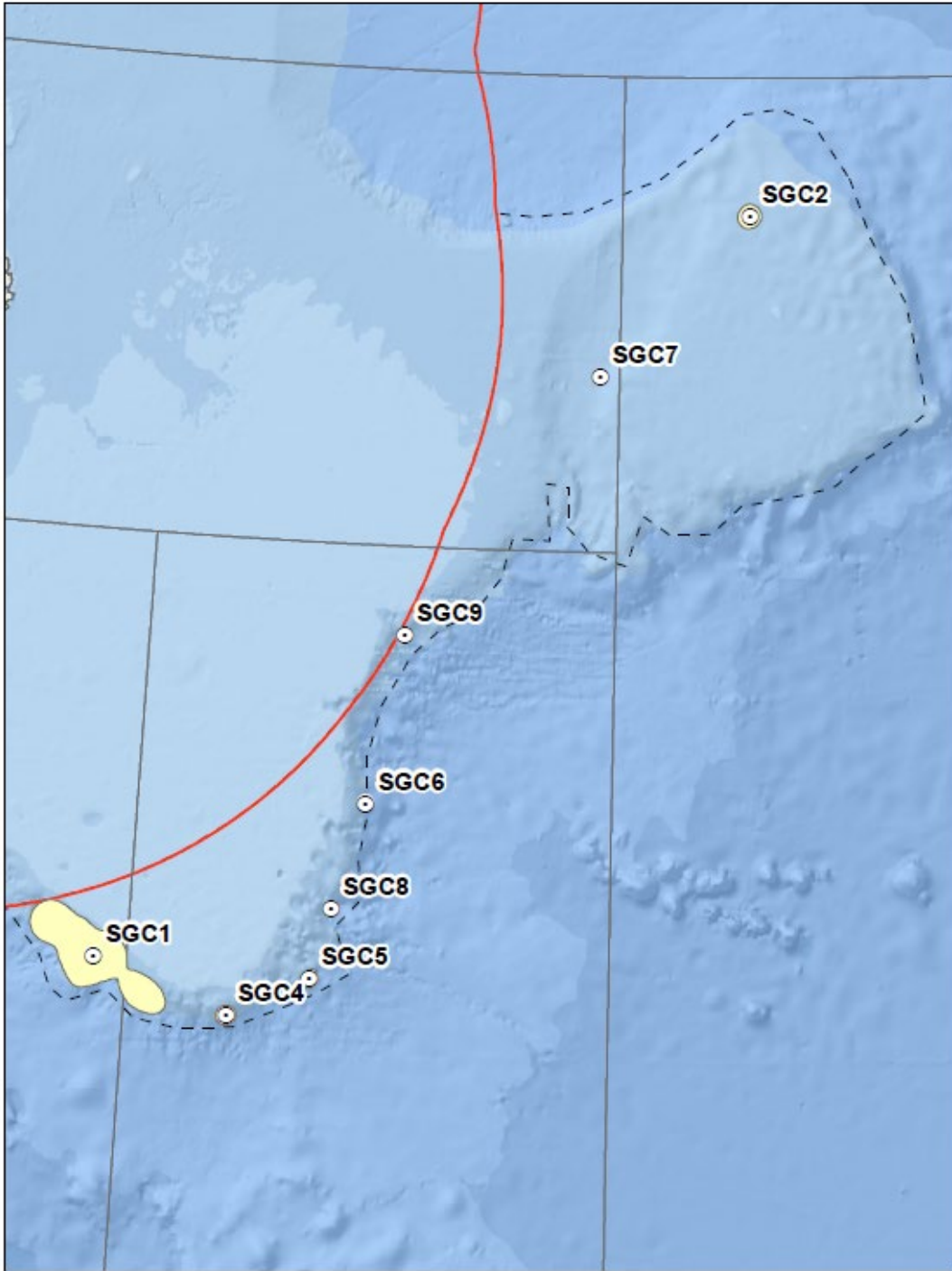
Figure 12. Location of the Small Gorgonian Coral (SGC) VMEs numbered according to VME area with SGC1 having the largest area (Table 11). VME polygons were produced following Kenchington et al. (2019). Dashed line represents the fishing footprint (~2000 m); red line indicates EEZ of Canada. NAD83 UTM 23 projection.
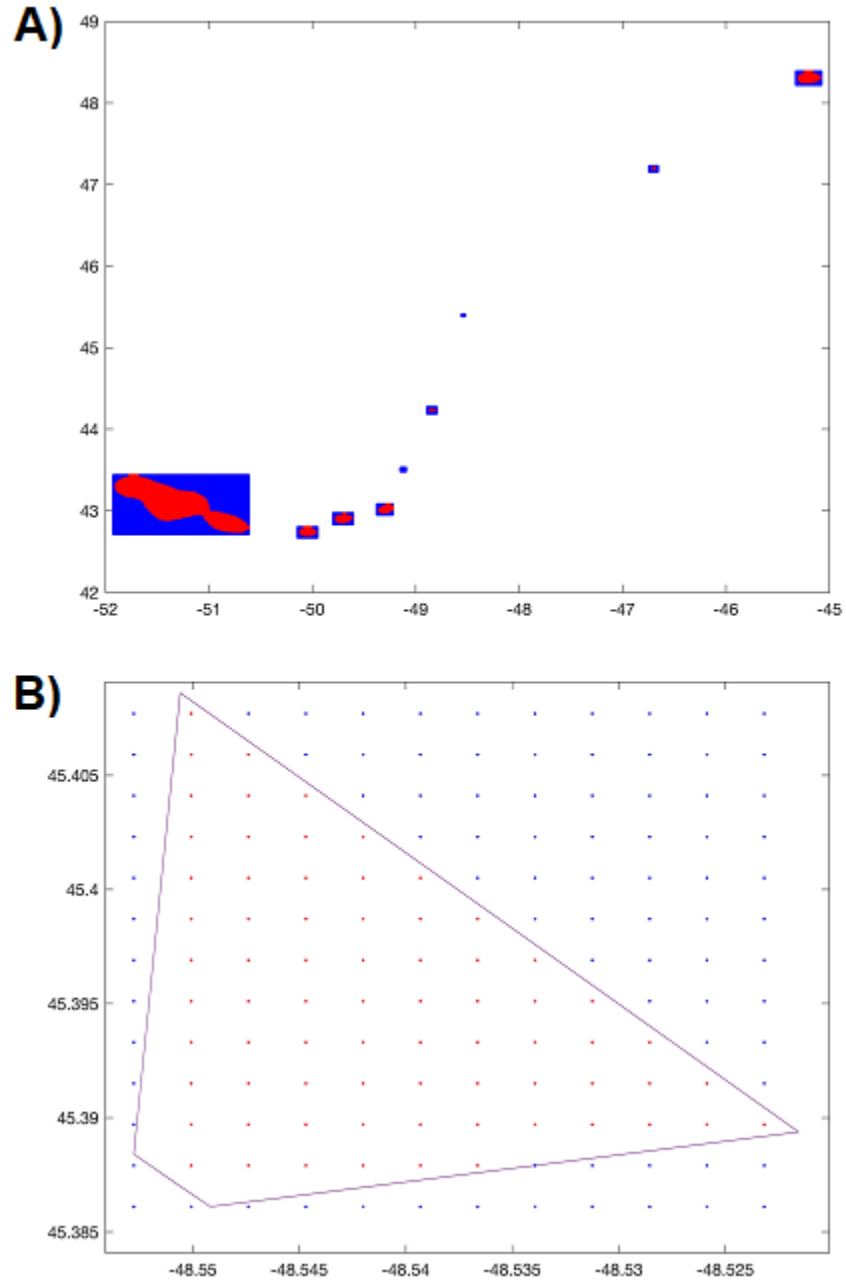
Figure 13. Steps showing the construction of grid cells for the particle seeding for the LPT analyses among small gorgonian coral VMEs. A) rectangles (red and blue) were placed over each small gorgonian coral VME polygon (red) within which B) a uniform grid with 1-km spacing was overlain and grid points falling within the small gorgonian coral VME polygons (red) were used to position particles to seed the analyses. Projection: NAD83 UTM 23.
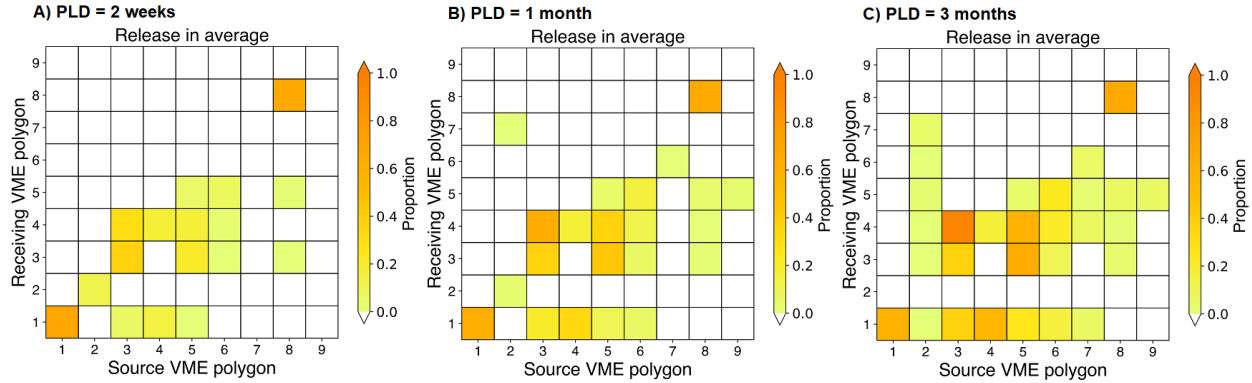
Figure 14. Connectivity matrices between the nine small gorgonian coral VME polygons for particles released for two weeks, one month and three months (PLD) using monthly-averaged currents as evaluated in Wang et al. (2020). The diagonal represents particle retention. Polygon numbers are as in Figure 12.

Table 11. Unidirectional (source to sink) nearest neighbour distances (km) calculated from centroid to centroid for the small gorgonian coral VME polygons in the NAFO Regulatory Area (numbered as in Figure 12) which showed connectivity (Figure 14). The mean nearest-neighbour distance for each polygon is shown.

			Source Small Gorgonian Coral VME Polygon								
		Polygon Area km²	SGC1	SGC2	SGC3	SGC4	SGC5	SGC6	SGC7	SGC8	SGC9
Sink Small Gorgonian Coral VME Polygon	SGC1	3669.3	---	750	133	110	165	237	583		
	SGC2	262.5		---							
	SGC3	184.1		695	---		36	163		82	
	SGC4	182.1		725	34	---	69	193	561	114	
	SGC5	147		668			---	140	507	56	271
	SGC6	48.1		532				---	369		
	SGC7	33.7		167					---		
	SGC8	10.2								---	
	SGC9	3.1									---
	Mean Nearest-Neighbour Distance (Centroid-Centroid)		0	590	84	110	90	183	505	84	271

Table 12. Unidirectional (source to sink) nearest neighbour distances (km) calculated from edge to edge for the small gorgonian coral VME polygons in the NAFO Regulatory Area (numbered as in Figure 12) which showed connectivity (Figure 14). The mean nearest-neighbour distance for each polygon is shown.

			Source Small Gorgonian Coral VME Polygon								
		Polygon Area km²	SGC1	SGC2	SGC3	SGC4	SGC5	SGC6	SGC7	SGC8	SGC9
Sink Small Gorgonian Coral VME Polygon	SGC1	3669.3	---	718	68	39	103	205	557		
	SGC2	262.5		---							
	SGC3	184.1		678	---		20	152		72	
	SGC4	182.1		708	17	---	54	181	550	104	
	SGC5	147		651			---	128	495	46	262
	SGC6	48.1		519				---	361		
	SGC7	33.7		154					---		
	SGC8	10.2								---	
	SGC9	3.1									---
	Mean Nearest-Neighbour Distance (Edge-Edge)		0	571	43	39	59	167	491	74	262

Table 13. Isolation/Proximity indices for the small gorgonian coral VME polygons in the NAFO Regulatory Area calculated using only the connections that were shown to be possible through the LPT modeling (Figure 14).

Distance Measurement Method	Mean Nearest-Neighbour Distance Over All Polygons Pairs	Proximity Index (PX)
Centroid-Centroid	307	
Edge-Edge	285	25.3

Black Coral

Connectivity modeling of the black corals has not previously been reported. The NAFO CEMs (NAFO, 2021) report *Stichopathes* sp., *Leiopathes* cf. *expansa*, *Leiopathes* sp., *Plumapathes* sp., *Bathypathes* cf. *patula*, *Parantipathes* sp., *Stauropathes arctica*, *Stauropathes* cf. *punctata*, and *Telopathes magna* as VME Indicator taxa, although some of these may be seamount species. Murillo et al. (2016) report the presence of *Stichopathes* sp. and *Stauropathes arctica* from the Flemish Cap and Grand Bank region. Wagner et al. (2011) have reviewed the reproductive biology of antipatharians. As for many deep-sea species very little is known and what we do know is based on small sample sizes. *Antipathes fiordensi*, a black coral species endemic to the south-western region of New Zealand, has been shown to have very restricted larval dispersal with highly philopatric larval settlement near the parent colonies (Miller et al., 1998). *In vitro* observations showed the larvae to be negatively buoyant with week swimming ability, however as none settled the crawling behaviour of the planulae was not observed (Miller, 1996). Similarly, there is very little data on the spawning season of black corals, and what is known has been extracted from oocyte size frequency distributions taken from specimens sampled at single points in time (Wagner et al., 2011). Those data suggest that there is a seasonality to reproduction with peak spawning times likely occurring during periods of warmer water temperatures, at least in shallow-water species, although female spawning may occur repeatedly in successive events (Wagner et al., 2011). Given this uncertainty, we have chosen a short PLD for the black coral connectivity modeling (2 weeks) and used the long-term average currents to mimic larval behaviour.
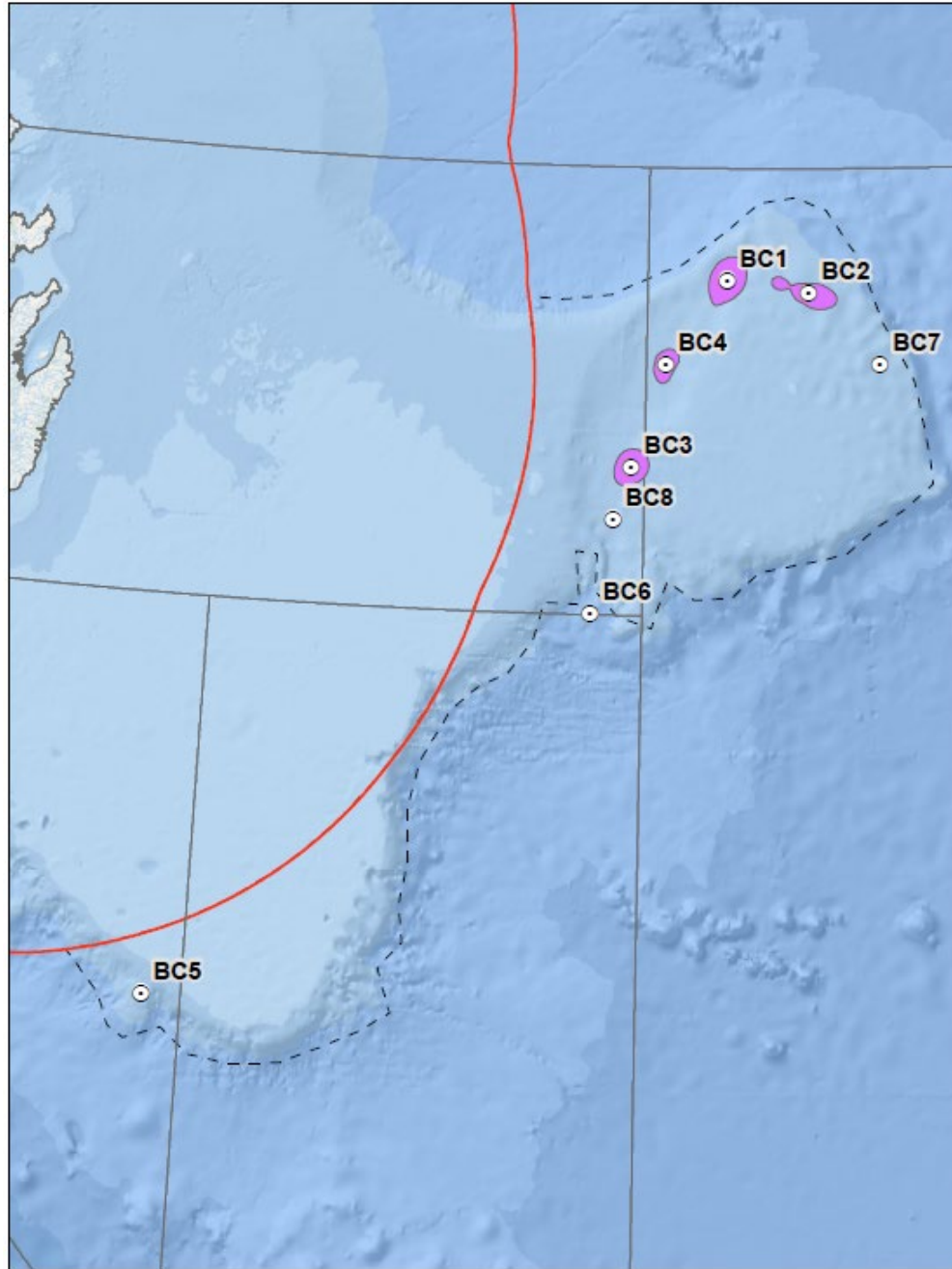
Figure 15. Location of the black coral (BC) VMEs numbered according to VME area with BC1 having the largest area (Table 14). VME polygons were produced following Kenchington et al. (2019). Dashed line represents the fishing footprint (~2000 m); red line indicates EEZ of Canada. NAD83 UTM 23 projection.
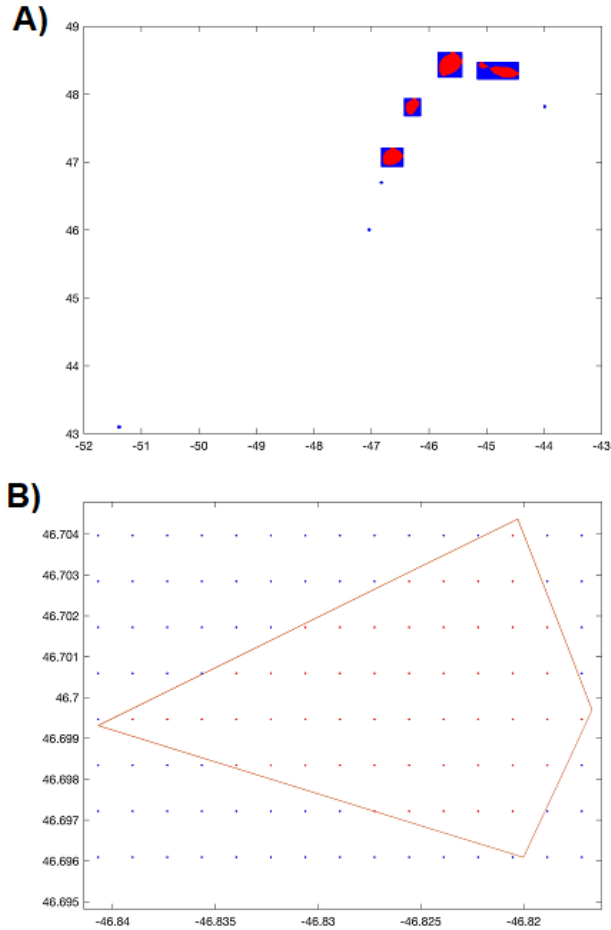
Figure 16. Steps showing the construction of grid cells for the particle seeding for the LPT analyses among black coral VMEs. A) rectangles (red and blue) were placed over each black coral VME polygon (red) within which B) a uniform grid with 1-km spacing was overlain and grid points falling within the black coral VME polygons (red) were used to position particles to seed the analyses. Projection: NAD83 UTM 23.
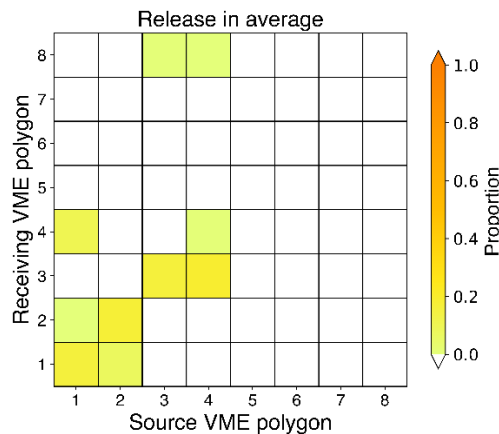
Figure 17. Connectivity matrices between the eight black coral VME polygons for particles released for two weeks (PLD) using monthly-averaged currents as evaluated in Wang et al. (2020). The diagonal represents particle retention. Polygon numbers are shown in Figure 15.

Particles for the LPT modeling were seeded uniformly inside the black coral VME polygons (Figure 15) as in Figure 16. Rectangles encapsulating each of the eight black coral VME polygons were constructed (Figure 16A) and a 1-km grid was overlain in each (Figure 16B). The projection NAD83 UTM 23 was used to construct all grids. The grid points falling within the black coral VME polygons were retained and used to seed particles for the LPT analyses (Figure 16B). A minimum of 50 particles per area was established and additional particles were randomly placed in black coral VME polygons.

We used averaged currents over the BNAM time frame (1990-2015) to release particles, as the spawning season for the black corals in the region is unknown. Particles were released from the sea bed and allowed to advect for two weeks, the latter a maximal estimate for pelagic larval duration (PLD) for the black corals which may settle over much shorter periods (see above). The connectivity matrices for PLD are shown in Figure 17. Only polygons showing connections were retained for the nearest neighbour distance calculations.

Table 14. Unidirectional (source to sink) nearest neighbour distances (km) calculated from centroid to centroid for the black coral VME polygons in the NAFO Regulatory Area (numbered as in Figure 15) which showed connectivity (Figure 17). The mean nearest-neighbour distance for each polygon is shown.

			Source Black Coral VME Polygon							
		Polygon Area km²	BC1	BC2	BC3	BC4	BC5	BC6	BC7	BC8
Sink Black Coral VME Polygon	BC1	882.5	---	66						
	BC2	699.4	66	---						
	BC3	643.8			---	87				
	BC4	400	84			---				
	BC5	2.1					---			
	BC6	1.2						---		
	BC7	1.1							---	
	BC8	0.8			44	131				---
	Mean Nearest-Neighbour Distance (Centroid-Centroid)		75	66	44	109	0	0	0	0

The nearest-neighbour distances in kilometres, calculated from centroid to centroid (Table 14) and from edge to edge (Table 15) for black coral polygons that have a strong likelihood of connecting with one another, as indicated by the LPT analyses are provided. As connections are only unidirectional from source to sink, the results are presented as a square matrix. Only 6 of the 56 possible connections (excluding retentions) were considered likely. Mean nearest-neighbour distances ranged from 0-109 km (centroid to centroid) and 0-86 km (edge to edge). The Proximity Index, PX, was slightly smaller than when all connections were considered (Table 16) being 108.9 previously (NAFO, 2020). Polygons BC1 and BC4 emerge as potential seed sources for two other polygons each (Figure 17) among VME polygons that are generally poorly connected.

Table 15. Unidirectional (source to sink) nearest neighbour distances (km) calculated from edge to edge for the black coral VME polygons in the NAFO Regulatory Area (numbered as in Figure 15) which showed connectivity (Figure 17). The mean nearest-neighbour distance for each polygon is shown.

			Source Black Coral VME Polygon							
		Polygon Area km²	BC1	BC2	BC3	BC4	BC5	BC6	BC7	BC8
Sink Black Coral VME Polygon	BC1	882.5	---	21						
	BC2	699.4	21	---						
	BC3	643.8			---	57				
	BC4	400	48			---				
	BC5	2.1					---			
	BC6	1.2						---		
	BC7	1.1							---	
	BC8	0.8			27	115				---
	Mean Nearest-Neighbour Distance (Edge-Edge)		35	21	27	86	0	0	0	0

Table 16. Isolation/Proximity indices for the black coral VME polygons in the NAFO Regulatory Area calculated using only the connections that were shown to be possible through the LPT modeling (Figure 17).

Distance Measurement Method	Mean Nearest-Neighbour Distance Over All Polygons Pairs	Proximity Index (PX)
Centroid-Centroid	80	
Edge-Edge	48	

Bryozoans

The only bryozoan indicator taxon listed in the NAFO CEMs is the feathery bryozoan, *Eucratea loricata* (NAFO, 2021). *Eucratea loricata* zooids form a tree-like colony up to 25 cm in height (Avant, 2004) and they occur generally at depths less than 100 m with Murillo et al. (2016) reporting its presence in 21 trawl sets from surveys done on Grand Bank in 2007 between 46-86 m. As for the other deep-sea VME indicator taxa, very little is known about the reproductive biology of this species. Most bryozoan larvae are lecithotrophic and only able to stay in the water column for a few hours (Ryland, 1974; Keough, 1989). Powell (1968) describes the breeding season for all species in the Arctic as from July-September which is likely also the case for *E. loricata*. Consequently, we have used a PLD of 2 weeks run for the Summer months, recognizing that this may produce more connections than would be realized with the short PLD thought to occur in these species.

Particles for the LPT modeling were seeded uniformly inside the bryozoan VME polygons (Figure 18) as in Figure 19. Rectangles encapsulating each of the seventeen bryozoan VME polygons were constructed (Figure 19A) and a 1-km grid was overlain in each (Figure 19B). The projection NAD83 UTM 23 was used to construct all grids. The grid points falling within the bryozoan VME polygons were retained and used to seed particles for the LPT analyses (Figure 19B). A minimum of 50 particles per area was established and additional particles were randomly placed in bryozoan VME polygons.
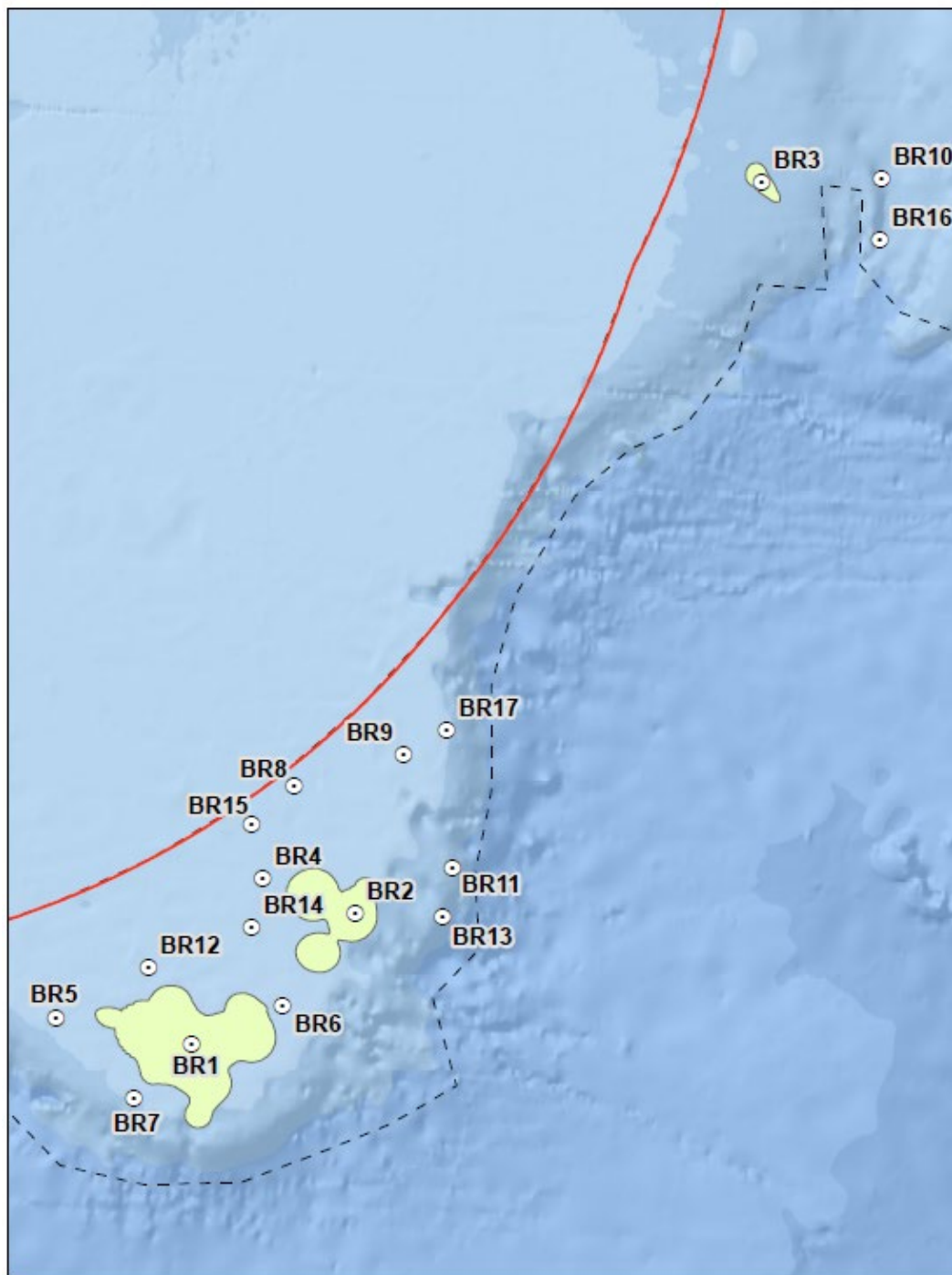
Figure 18. Location of the bryozoan (BR) VMEs numbered according to VME area with BR1 having the largest area (Table 17). VME polygons were produced following Kenchington et al. (2019). NAD83 UTM 23 projection.
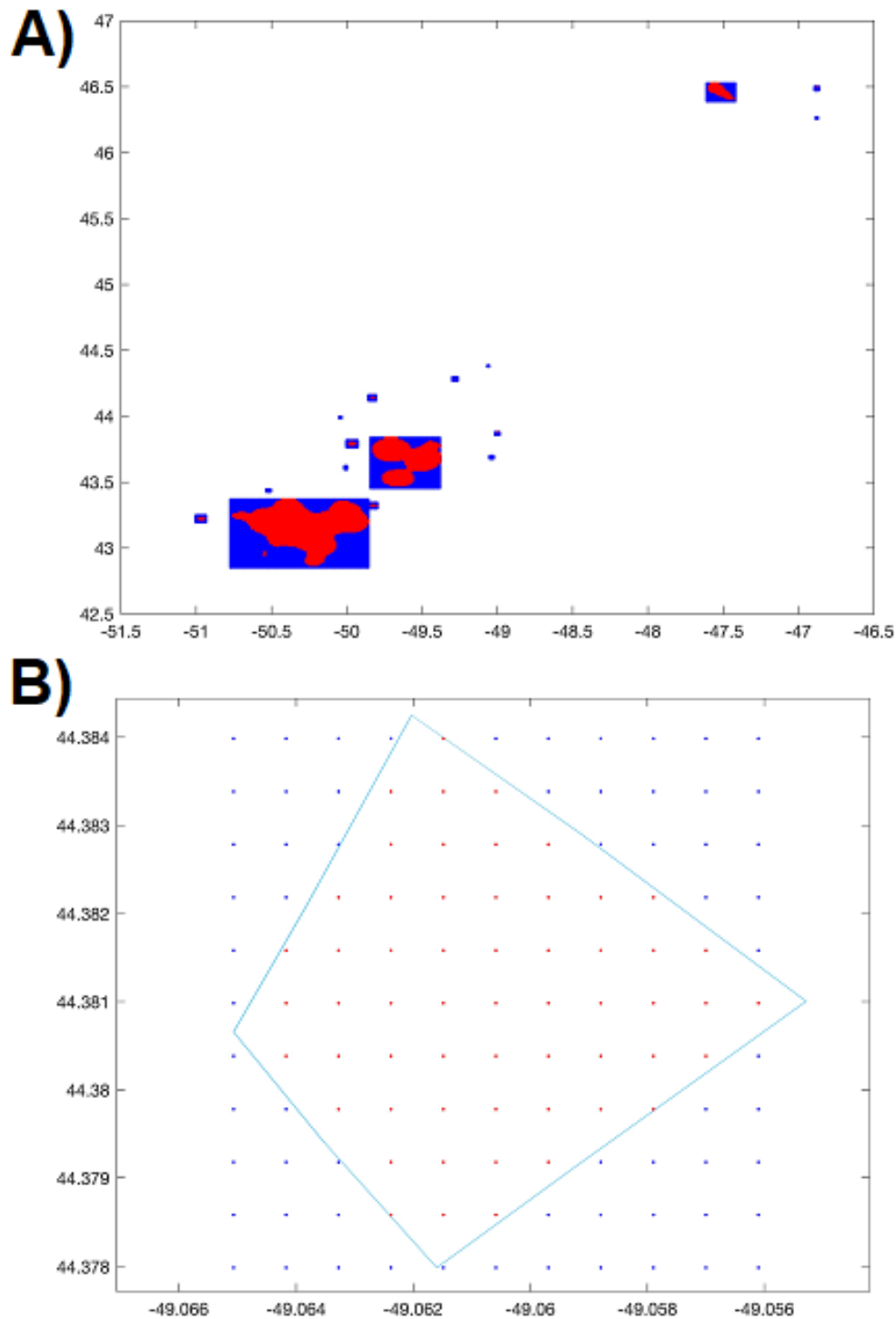
Figure 19. Steps showing the construction of grid cells for the particle seeding for the LPT analyses among bryozoan VMEs. A) rectangles (red and blue) were placed over each bryozoan VME polygon (red) within which B) a uniform grid with 1-km spacing was overlain and grid points falling within the bryozoan VME polygons (red) were used to position particles to seed the analyses. Projection: NAD83 UTM 23.

We used averaged currents for each of July, August and September over the BNAM time frame (1990-2015) to release particles, as this best reflects the bryozoan the spawning season. Particles were released from the sea bed and allowed to advect for two weeks, the latter a maximal estimate for pelagic larval duration (PLD) for the bryozoans which may settle over much shorter periods (see above). The connectivity matrices for PLD are shown in Figure 20. Only polygons showing connections were retained for the nearest neighbour distance calculations.
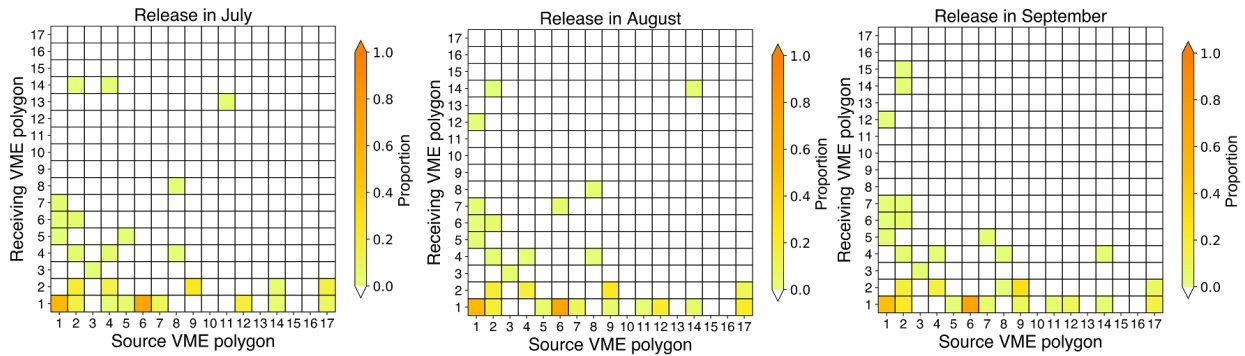
Figure 20. Connectivity matrices between the seventeen bryozoan VME polygons for particles released for two weeks (PLD) using monthly-averaged currents for July, August and September, the presumed spawning season for these species. The diagonal represents particle retention. Polygon numbers are shown in Figure 18.

The nearest-neighbour distances in kilometres, calculated from centroid to centroid (Table 17) and from edge to edge (Table 18) for bryozoan VME polygons that have a strong likelihood of connecting with one another, as indicated by the LPT analyses are provided. As connections are only unidirectional from source to sink, the results are presented as a square matrix. Only 30 of the 272 possible connections (excluding retentions) were considered likely. Mean nearest-neighbour distances ranged from 0-126 km (centroid to centroid) and 0-103 km (edge to edge). The Proximity Index, PX, was slightly smaller than when all connections were considered (Table 19) being 717.1 previously (NAFO, 2020). Polygons BR1 and BR2 on the Tail of Grand Bank emerge as potential seed sources for a number of other polygons each (Figure 20) among VME polygons that are generally poorly connected.

Table 17. Unidirectional (source to sink) nearest neighbour distances (km) calculated from centroid to centroid for the bryozoan VME polygons in the NAFO Regulatory Area (numbered as in Figure 18) which showed connectivity (Figure 20). The mean nearest-neighbour distance for each polygon is shown. Columns represent Source Polygons; Rows represent Sink (Receiving) Polygons.

Sink VME	Polygon Area km²	BR1	BR2	BR3	BR4	BR5	BR6	BR7	BR8	BR9	BR10	BR11	BR12	BR13	BR14	BR15	BR16	BR17
												Source Bryozoan VME Polygon						
BR1	2243.9	---	86		74	57	40	33		148		130	36		54			167
BR2	1006		---		41				58	69					43			84
BR3	125.7			---														
BR4	25.8		41		---				40						21			
BR5	24.2	57				---		46										
BR6	17.2	40	49				---											
BR7	13.4	33	119				72	---										
BR8	12.8								---									
BR9	5.4									---								
BR10	4.6										---							
BR11	4.3											---						
BR12	2.7	36											---					
BR13	2.4											20		---				
BR14	1.9		43		21										---			
BR15	0.5		56													---		
BR16	0.4																---	
BR17	0.3																	---
Mean Nearest-Neighbour Distance (Centroid-Centroid)		42	66	0	45	57	56	40	49	109	0	75	36	0	39	0	0	126

Table 18. Unidirectional (source to sink) nearest neighbour distances (km) calculated from edge to edge for the bryozoan VME polygons in the NAFO Regulatory Area (numbered as in Figure 18) which showed connectivity (Figure 20). The mean nearest-neighbour distance for each polygon is shown. Columns represent Source Polygons; Rows represent Sink (Receiving) Polygons.

Sink VME	Polygon Area km²	Source Bryozoan VME Polygon																
		BR1	BR2	BR3	BR4	BR5	BR6	BR7	BR8	BR9	BR10	BR11	BR12	BR13	BR14	BR15	BR16	BR17
BR1	2243.9	---	22		45	13	4	6		116		94		9	26			136
BR2	1006		---		8				32	52					17			69
BR3	125.7			---														
BR4	25.8		8		---				35						16			
BR5	24.2	13				---		41										
BR6	17.2	4	16				---											
BR7	13.4	6	86				67	---										
BR8	12.8								---									
BR9	5.4									---								
BR10	4.6										---							
BR11	4.3											---						
BR12	2.7	9											---					
BR13	2.4											18		---				
BR14	1.9		17		16										---			
BR15	0.5		27													---		
BR16	0.4																---	
BR17	0.3																	---
Mean Nearest-Neighbour Distance (Edge-Edge)		8	29	0	23	13	36	24	34	84	0	56	0	9	20	0	0	103

Table 19. Isolation/Proximity indices for the bryozoan VME polygons in the NAFO Regulatory Area calculated using only the connections that were shown to be possible through the LPT modeling (Figure 20).

Distance Measurement Method	Mean Nearest-Neighbour Distance Over All Polygons Pairs	Proximity Index (PX)
Centroid-Centroid	61	
Edge-Edge	34	699.5

Sea Squirts *(Boltenia ovifera)*

Connectivity modeling of the sea squirts, *Boltenia ovifera*, has not previously been reported. The reproductive season of this species was described for the first time by Lacalli (1980) who reported a January and February spawning season in the Bay of Fundy, Canada. The larvae were lecithotrophic (non-feeding) with a very short PLD: "The larva does not swim actively; it appears instead to be carried passively by surface currents for a brief period after hatching, while the tail generates only weak and sporadic twitches." (Lacalli, 1980). Consequently, we used the monthly-averaged currents for January and February with PLD of 2 weeks for this VME Indicator.

The CEM reports a second species in this group, the sea peach *Halocynthia aurantium* (NAFO, 2021). This species may be misrepresented as it is a species of the North Pacific. More likely the species present in the NRA is *H. pyriformis* (Ma et al., 2017). The sea peach *Halocynthia pyriformis*, is a dominant member of the benthic community in the Bay of Fundy, where it occurs in densities of up to 60 individuals m^{-2} (Armsworthy et al., 2001). If *H. pyriformis* is present in the NRA it likely has similar reproductive traits to its Pacific congeners whose larvae metamorphose quickly, with oral and atrial siphons of settled juveniles appearing 23 days post fertilization at 11°C. Larval development is slower at low temperatures and more rapid at high temperatures (Kim, 2020). Murillo et al. (2016) recorded the presence of *Halocynthia* sp. 1 in one trawl from the Grand Bank during a detailed examination of the 2007 trawl catch from the Spanish surveys. Therefore, if present, the species is likely not common. Given the uncertainties surrounding the presence of this taxon in the NRA and the lack of direct information on its reproduction, we have used the reproductive traits of *Boltenia ovifera* to inform the LPT models.

Particles for the LPT modeling were seeded uniformly inside the sea squirt VME polygons (Figure 21) as in Figure 22. Rectangles encapsulating each of the eighteen sea squirt VME polygons were constructed (Figure 22A) and a 1-km grid was overlain in each (Figure 22B). The projection NAD83 UTM 23 was used to construct all grids. The grid points falling within the sea squirt VME polygons were retained and used to seed particles for the LPT analyses (Figure 22B). A minimum of 50 particles per area was established and additional particles were randomly placed in sea squirt VME polygons.

We used averaged currents for each of January and February over the BNAM time frame (1990-2015) to release particles, as this best reflects the *B. ovifera* the spawning season. Particles were released from the sea bed and allowed to advect for two weeks, the latter a maximal estimate for pelagic larval duration (PLD) for the species which may settle over much shorter periods (see above). The connectivity matrices for PLD are shown in Figure 23. Only polygons showing connections were retained for the nearest neighbour distance calculations.
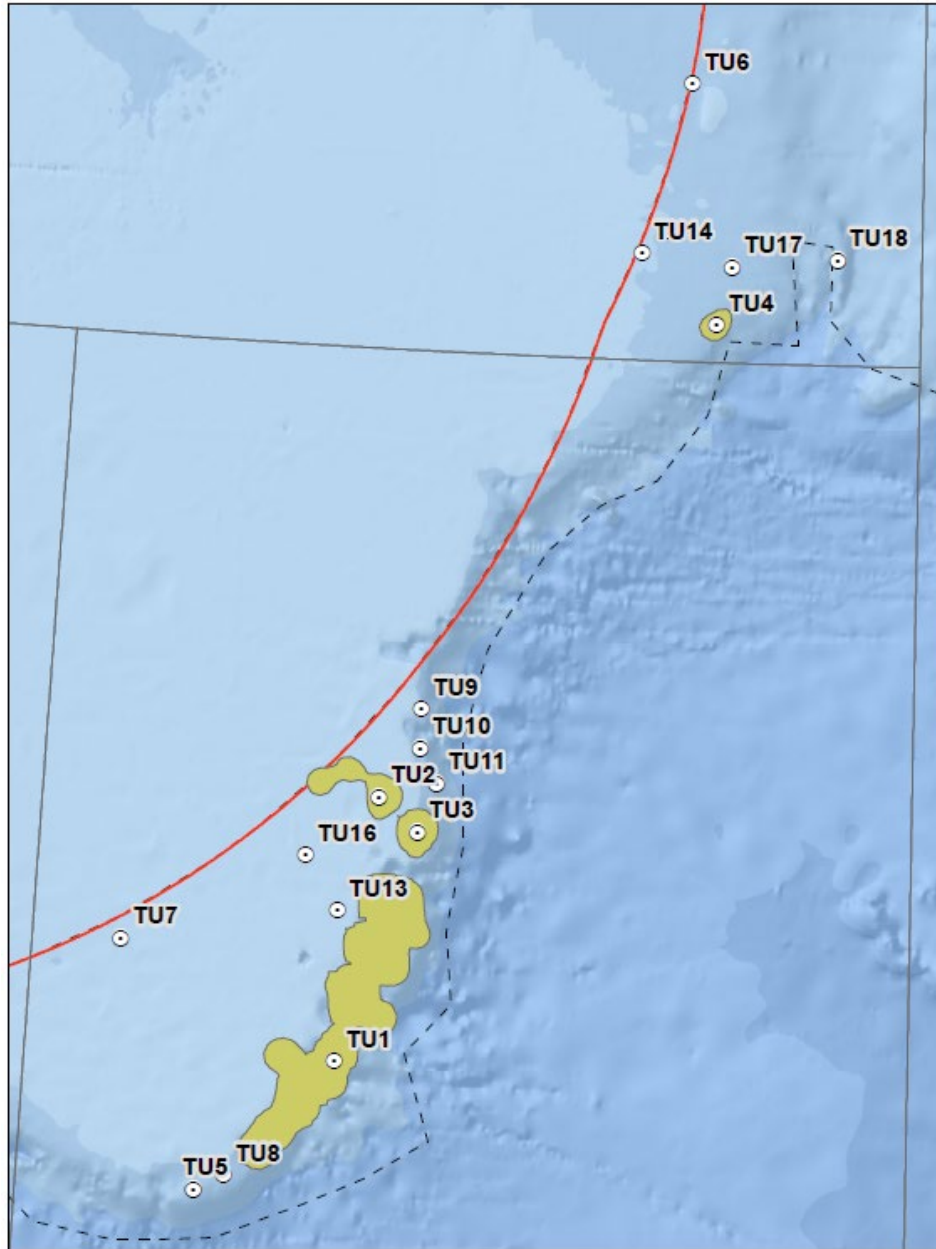
Figure 21. Location of the Sea Squirts (TU) VMEs numbered according to VME area with TU1 having the largest area (Table 20). VME polygons were produced following Kenchington et al. (2019). NAD83 UTM 23 projection.
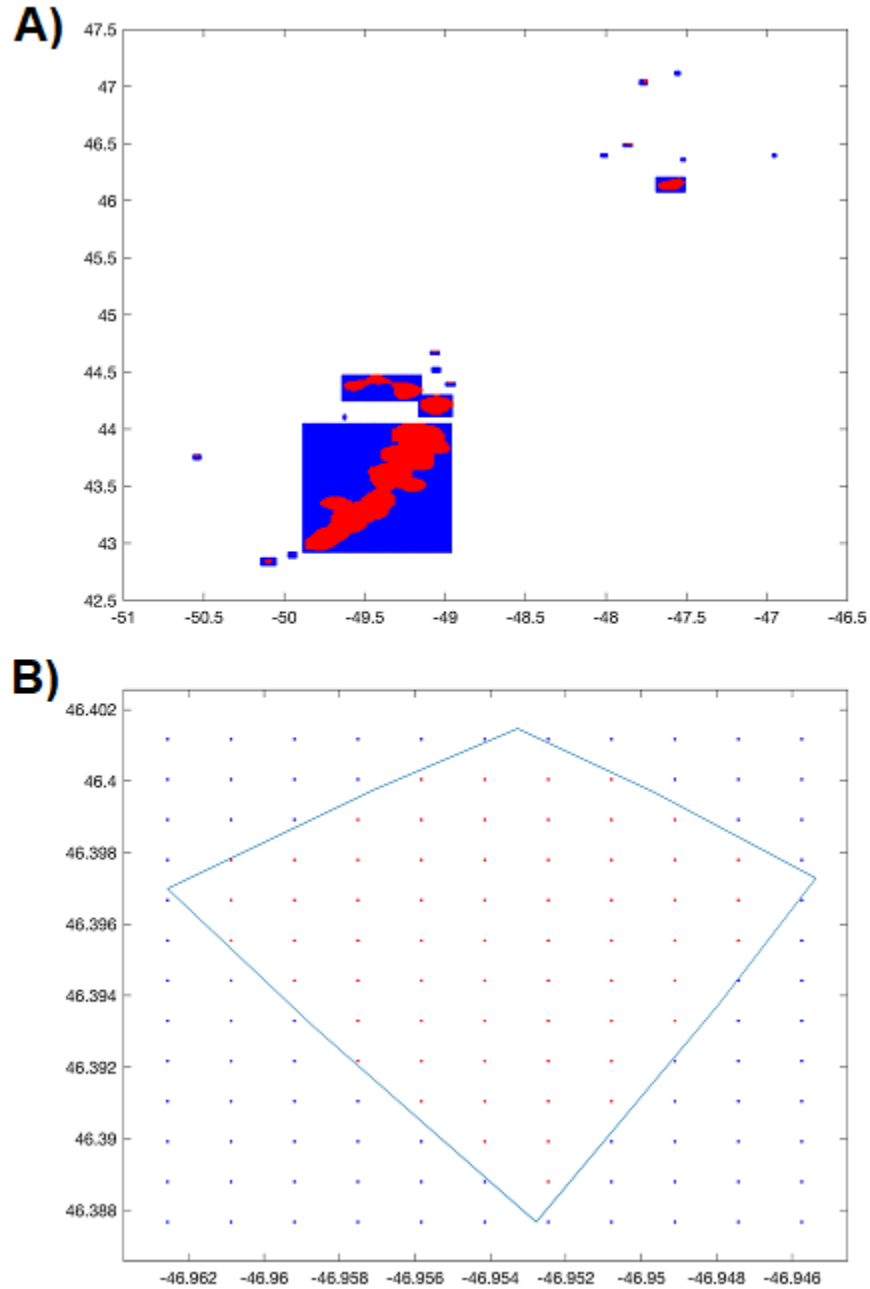
Figure 22. Steps showing the construction of grid cells for the particle seeding for the LPT analyses among sea squirt (Boltenia) VMEs. A) rectangles (red and blue) were placed over each sea squirt VME polygon (red) within which B) a uniform grid with 1-km spacing was overlain and grid points falling within the sea squirt VME polygons (red) were used to position particles to seed the analyses. Projection: NAD83 UTM 23.
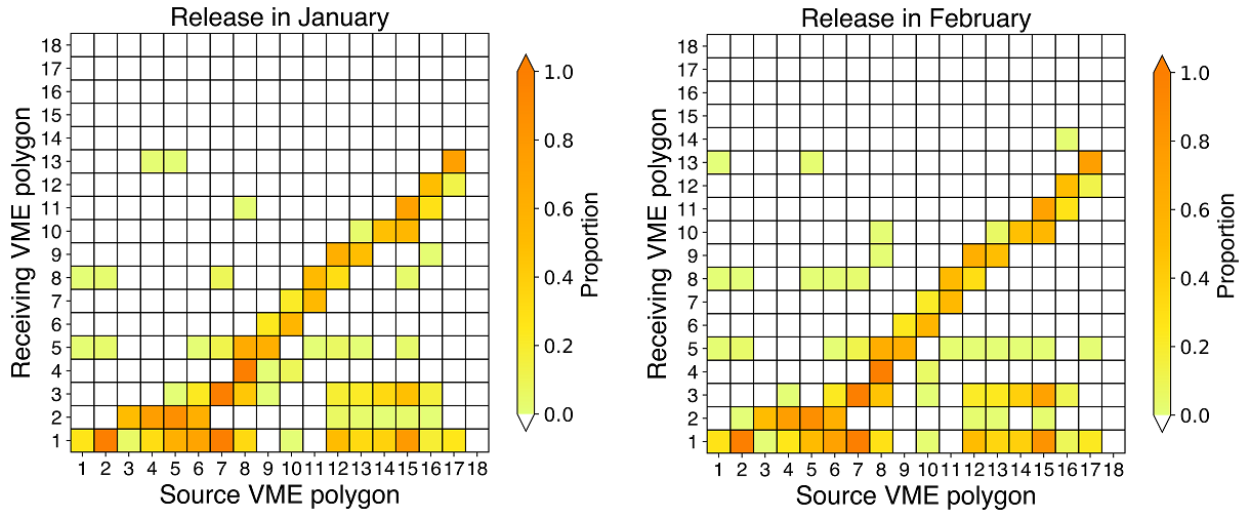
Figure 23. Connectivity matrices between the eighteen sea squirt VME polygons for particles released for two weeks (PLD) using monthly-averaged currents for January and February, the presumed spawning season for these species. The diagonal represents particle retention. Polygon numbers are shown in Figure 21.

The nearest-neighbour distances in kilometres, calculated from centroid to centroid (Table 20) and from edge to edge (Table 21) for sea squirt VME polygons that have a strong likelihood of connecting with one another, as indicated by the LPT analyses are provided. As connections are only unidirectional from source to sink, the results are presented as a square matrix. Only 80 of the 306 possible connections (excluding retentions) were considered likely. Mean nearest-neighbour distances ranged from 0-415 km (centroid to centroid) and 0-392 km (edge to edge). The Proximity Index, PX, was smaller than when all connections were considered (Table 22) being 801.5 previously (NAFO, 2020). Polygons TU8, TU15 and TU16 were particularly well connected to other polygons with seven connections each. These emerge as potential seed sources for a number of other polygons each (Figure 23) among VME polygons that are generally better connected than some of the others with only TU18 unconnected to another polygon.

Table 20. Unidirectional (source to sink) nearest neighbour distances (km) calculated from centroid to centroid for the sea squirt (Boltenia) VME polygons in the NAFO Regulatory Area (numbered as in Figure 21) which showed connectivity (Figure 23). The mean nearest-neighbour distance for each polygon is shown. Columns represent Source Polygons; Rows represent Sink (Receiving) Polygons.

Sink VME Polygon	VME Area km²	Source Sea Squirt (Boltenia) VME Polygon																	
		TU1	TU2	TU3	TU4	TU5	TU6	TU7	TU8	TU9	TU10	TU11	TU12	TU13	TU14	TU15	TU16	TU17	TU18
TU1	3167.7	---	111	101	343	79	431	102	66		134		370	62	358	444	86	367	
TU2	435.1		---	22	240	179	322						263	50	250	336	39		
TU3	259.6			---	243	174	330	130	163	51	35		270	46	257	343	47		
TU4	126.9				---				406	200	214								
TU5	27.3	79	179			---	501	108	14	220		195	443	130	429	516		442	
TU6	8.7						---			282	297								
TU7	8.3							---			146	145							
TU8	8.2	66	169			14	491	107	---			184	432			505			
TU9	6.3								209	---			223	90				77	
TU10	6.3								194		---			75	224	311			
TU11	6.0								184			---				322	62		
TU12	4.2												---				299	30	
TU13	3.2	62			288	130								---				312	
TU14	2.7														---		285		
TU15	2.2															---			
TU16	1.8																---		
TU17	1.1																	---	
TU18	1.0																		---
Mean Nearest-Neighbour Distance (Centroid-Centroid)		69	153	62	279	115	415	112	177	188	165	175	334	76	304	397	128	288	0

Table 21. Unidirectional (source to sink) nearest neighbour distances (km) calculated from edge to edge for the sea squirt (Boltenia) VME polygons in the NAFO Regulatory Area (numbered as in Figure 21) which showed connectivity (Figure 23). The mean nearest-neighbour distance for each polygon is shown. Columns represent Source Polygons; Rows represent Sink (Receiving) Polygons.

Sink VME Polygon	VME Area km²	Source Sea Squirt (Boltenia) VME Polygon																	
		TU1	TU2	TU3	TU4	TU5	TU6	TU7	TU8	TU9	TU10	TU11	TU12	TU13	TU14	TU15	TU16	TU17	TU18
TU1	3167.7	---	23	9	255	19	347	73	6		51		288	6	275	362	24	285	
TU2	435.1		---	2	224	168	310						253	40	240	326	24		
TU3	259.6			---	227	161	318	120	151	40	23		259	36	246	333	38		
TU4	126.9				---				398	192	205								
TU5	27.3	19	168			---	496	103	9	215		191	438	126	425	512		438	
TU6	8.7						---			278	293								
TU7	8.3							---			143	142							
TU8	8.2	6	158			9	487	103	---			181	429			503			
TU9	6.3								206	---			220	88			74		
TU10	6.3								190		---			72	222	309			
TU11	6.0								181			---				320	59		
TU12	4.2												---				296	28	
TU13	3.2	6			281	126								---				311	
TU14	2.7														---		283		
TU15	2.2															---			
TU16	1.8																---		
TU17	1.1																	---	
TU18	1.0																		---
Mean Nearest-Neighbour Distance (Edge-Edge)		10	116	6	247	97	392	100	163	181	143	171	315	61	282	381	114	266	0

Table 22. Isolation/Proximity indices for the sea quirt (Boltenia) VME polygons in the NAFO Regulatory Area calculated using only the connections that were shown to be possible through the LPT modeling (Figure 23).

Distance Measurement Method	Mean Nearest-Neighbour Distance Over All Polygons Pairs	Proximity Index (PX)
Centroid-Centroid	214	
Edge-Edge	194	682.9

Application to the New Closed Areas in the NAFO Regulatory Area (Effective 1 January 2022)

The results of the analyses applied to the new NAFO closed areas approved at the 2021 Annual General Meeting are shown in Tables 23 and 24. The distances between the closed areas (Figure 24) ranged from 31 to 842 km centroid to centroid, and 11 to 775 km edge to edge (Table 23). Using the distances from centroid to centroid, shown in the lower diagonal of Table 23, the values for the mean nearest-neighbour distance over all polygons and the average nearest neighbor ratio are provided in Table 24. The values for the mean nearest-neighbour centroid to centroid distance over all polygons (Table 23) and PX are provided for the edge-edge distances (Table 24). The establishment of the new closures did not change the edge-edge distance range or mean and only slightly changed the centroid-centroid distance, however PX was increased from 452 to 783. PX is larger when the polygons are surrounded by larger and/or closer polygons and decreases as polygons become smaller and/or sparser (Gustafson and Parker, 1994). The increase here is likely due to the increase in size of the closed areas which combine some of the previous smaller closures.

Table 23. Nearest neighbour distances (km) calculated from centroid to centroid (below diagonal, shaded) and from nearest edges (above diagonal) for the closed areas in the NAFO Regulatory Area (numbered as in Figure 24). The mean nearest-neighbour distance for each closed area, as a measure of relative isolation, is shown below the rows for the centroid to centroid distances and to the right of columns for the nearest edges distances. Closed areas are numbered according to the NAFO Conservation and Enforcement Measures. All calculations were performed using NAD83 UTM 23 projection.

Area No.	Description	Polygon Area km²	Area 1	Area 2	Area 3	Area 4	Area 5	Area 6	Area 7	Area 10	Area 11	Area 12	Area 13	Area 14a	Area 14b	3O	Mean Nearest-Neighbour Distance (Edge-Edge)
Area 1	Tail of the Bank	172	---	55	254	454	532	470	518	427	386	480	299	525	514	211	394
Area 2	Flemish Pass	5,771	263	---	52	202	230	127	176	83	43	137	58	212	214	284	144
Area 3	Beothuk Knoll	308	286	85	---	178	254	259	268	199	159	244	27	250	236	497	221
Area 4	E Flemish Cap	1,358	510	287	228	---	48	229	122	205	187	195	133	72	36	697	212
Area 5	NE Flemish Cap	2,879	594	335	316	169	---	80	11	127	169	57	205	12	10	775	193
Area 6	Sackville Spur	987	549	288	305	261	136	---	40	32	81	16	221	147	174	686	197
Area 7	N Flemish Cap	1,053	564	302	294	186	48	90	---	58	108	15	223	40	67	753	184
Area 10	NW Flemish Cap	527	472	210	230	231	162	78	116	---	18	11	159	148	165	657	176
Area 11	NW Flemish Cap	220	423	160	179	219	191	130	150	52	---	69	121	163	169	619	176
Area 12	NW Flemish Cap	511	555	292	301	234	104	32	58	85	132	---	202	114	141	712	184
Area 13	Beothuk Knoll	338	333	104	49	186	267	262	245	189	141	255	---	200	186	542	198
Area 14a	NE Flemish Cap	50	551	300	268	105	65	170	85	166	177	140	219	---	17	768	205
Area 14b	NE Flemish Cap	104	539	294	254	74	95	196	114	183	186	167	206	31	---	757	207
3O	3O Coral Closure	3,694	269	508	548	775	842	774	807	702	658	787	593	806	798	---	612
Mean Nearest-Neighbour Distance (Centroid-Centroid)			455	264	257	267	256	252	235	221	215	242	235	237	241	682	

Table 24. Isolation/Proximity indices for the VME closures in the NAFO Regulatory Area.

| Distance Measurement Method	Mean Nearest-Neighbour Distance Over All Polygons Pairs	Nearest Neighbour Ratio	Proximity Index (PX)
Centroid-Centroid	290	1.287498 p-value: 0.040	
Edge-Edge	236		782.96
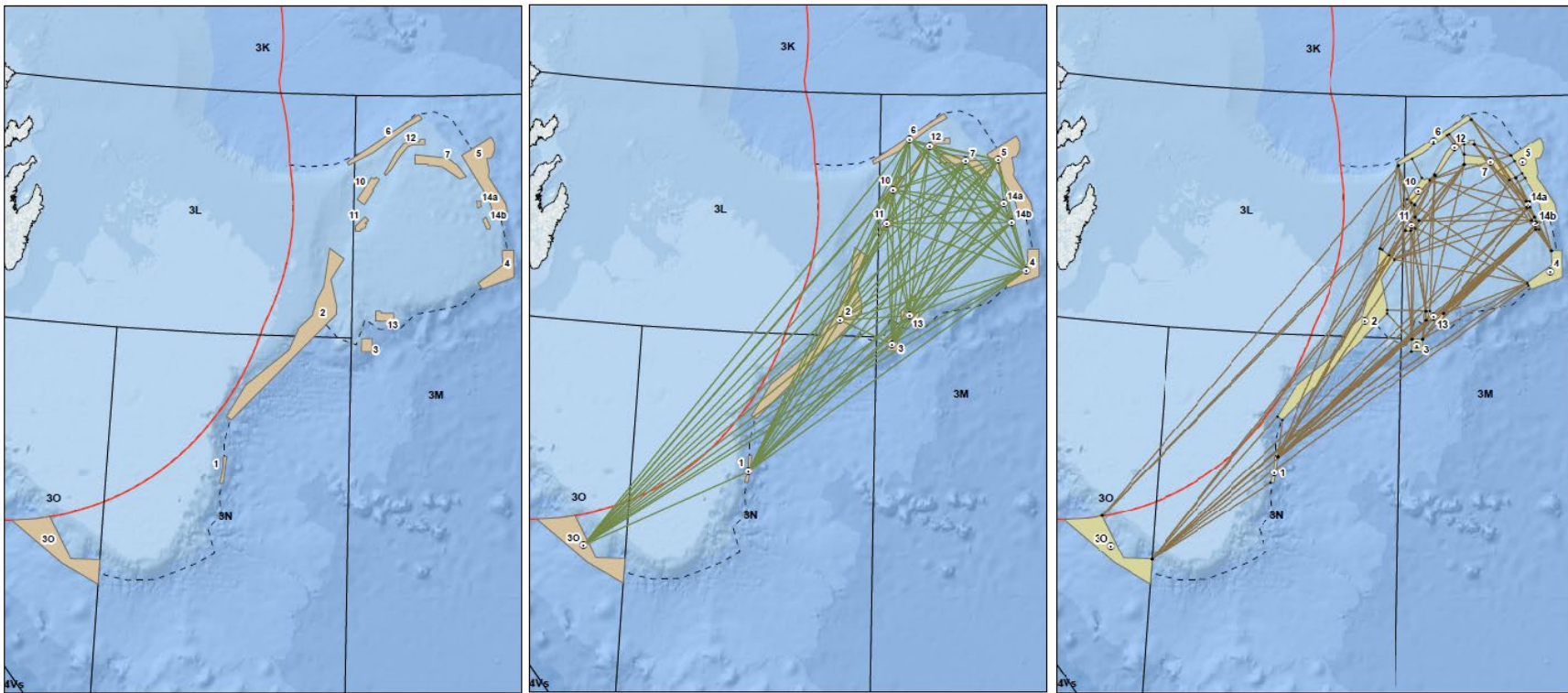
Figure 24. Nearest neighbour distance lines between areas closed to protect coral and sponge in the NRA (Left panel) calculated from centroid to centroid (Middle panel) and from the nearest edge (Right panel). NAD83 UTM 23 projection.

Modifications to Connections Among the New Closed Areas Based on Particle Tracking Modeling

Connectivity among the new closed areas was applied as for the various VME polygon examples above. We assessed connectivity among the new closed areas using average monthly currents for the summer and fall (summer refers to monthly averaged currents for July, Aug, Sep; fall refers to monthly averaged currents for Oct, Nov, Dec). The currents were averaged over the long term time period of the data for each month, 1995-2015. The 3-D LPT models were seeded on the bottom and the diffusivity constant K_h=100 m s^{-1} applied (Wang et al., 2020). Models were run for 2 weeks, 1 month and 3 months given the uncertainty in the reproductive biology of all of the VME Indicators present (Table 25). Seeding of particles was the same as for the various VME polygons and is illustrated in Figure 25. The results are shown in Figure 26. As expected, there are more connections made with the longer model runs (3 months) but given the uncertainties surrounding the reproductive biology and larval ecology of these VME Indicators we have used a conservative approach and accepted all connections made under all of the model simulations (Figures 26, 27). Tables 26 and 27 provide the modifications to the distances shown in Tables 23 and 24 through removal of unlikely connections.
Removal of unlikely connections resulted in a similar average distance edge-edge and a reduced average centroid-centroid distance. PX was much reduced from 782.96 when all connections are considered (Table 24) to 660.60 when unlikely connections are removed (Table 28). Every closed area showed some degree of retention while 823 of 182 possible connections were identified in the LPT modeling (46%).

Table 25. Description of the new NAFO Closed Areas with the VME taxa under protection.

| Description of Area	Closed Area Number	VME Type
Tail of the Bank	1	Sponge
Flemish Pass / Eastern Canyon	2	Sponge, Sea pen, Large and Small Gorgonian Corals, Boltenia, Black Coral
Beothuk Knoll	3	Sponge
Eastern Flemish Cap	4	Sponge, Large Gorgonian Corals
Northeast Flemish Cap	5	Sponge, Large Gorgonian Corals
Sackville Spur	6	Sponge
Northern Flemish Cap	7	Sea pen, Black Coral, Small Gorgonian Coral
Northwest Flemish Cap	10	Sea pen, *Asconema* Sponge
Northwest Flemish Cap	11	Sea pen
Northwest Flemish Cap	12	Sea pen, Black Corals
Beothuk Knoll	13	Large Gorgonian Corals
Northeast Flemish Cap	14a	Sea pen, Black Coral
Northeast Flemish Cap	14b	Sea pen
3O Coral Closure	3O	?
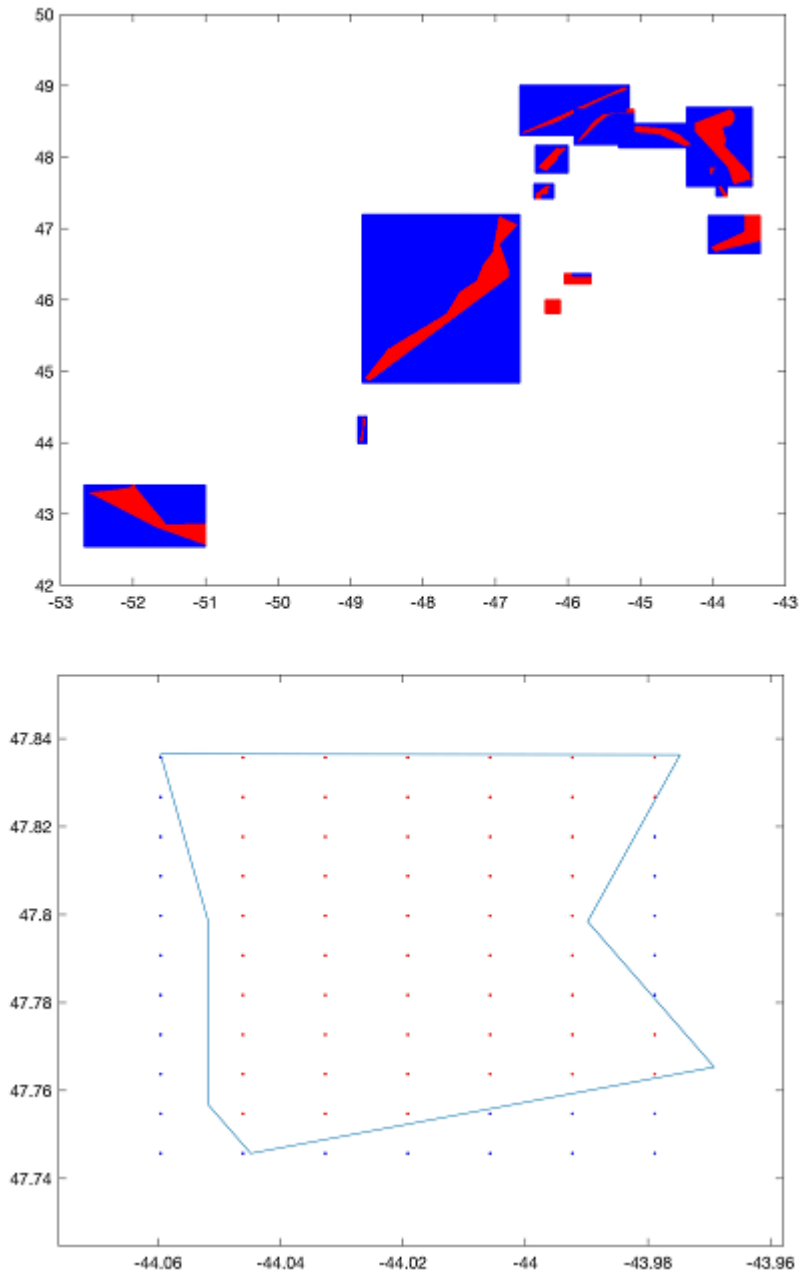
Figure 25. Steps showing the construction of grid cells for the particle seeding for the LPT analyses among the new NAFO Closed Areas which come into effect 1 January 2022. A) rectangles (red and blue) were placed over each closed area (red) within which B) a uniform grid with 1-km spacing was overlain and grid points falling within the sponge VME polygons were used to position particles to seed the analyses. Projection: NAD83 UTM 23.
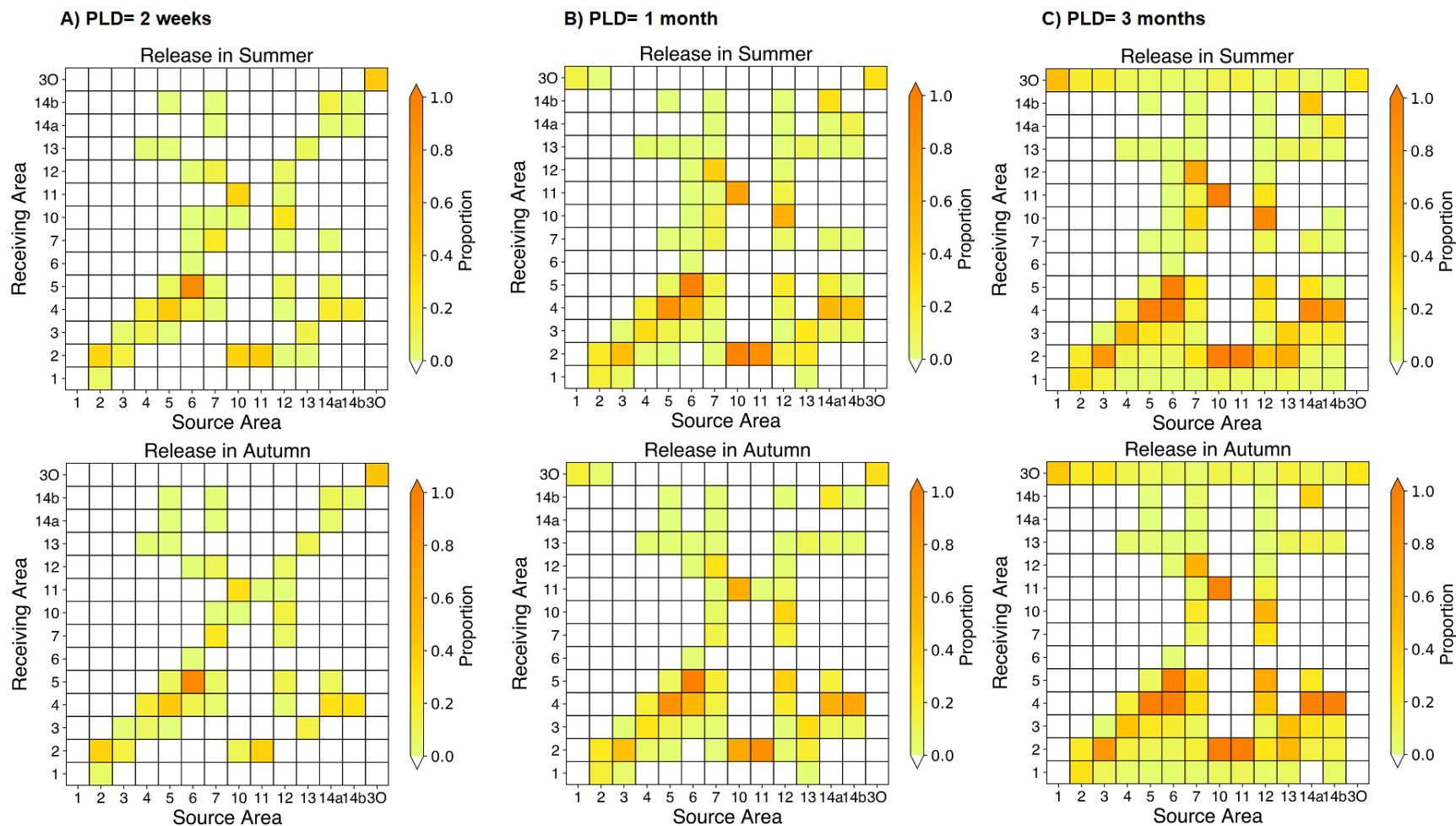
Figure 26. Connectivity matrices between NAFO Closed Areas in the Summer and Autumn for each of the pelagic larval durations (PLD) simulated in Wang et al. (2020) to reflect VME larval time in the water column. The diagonal represents particle retention. Closed Area numbers are shown in Figure 24.
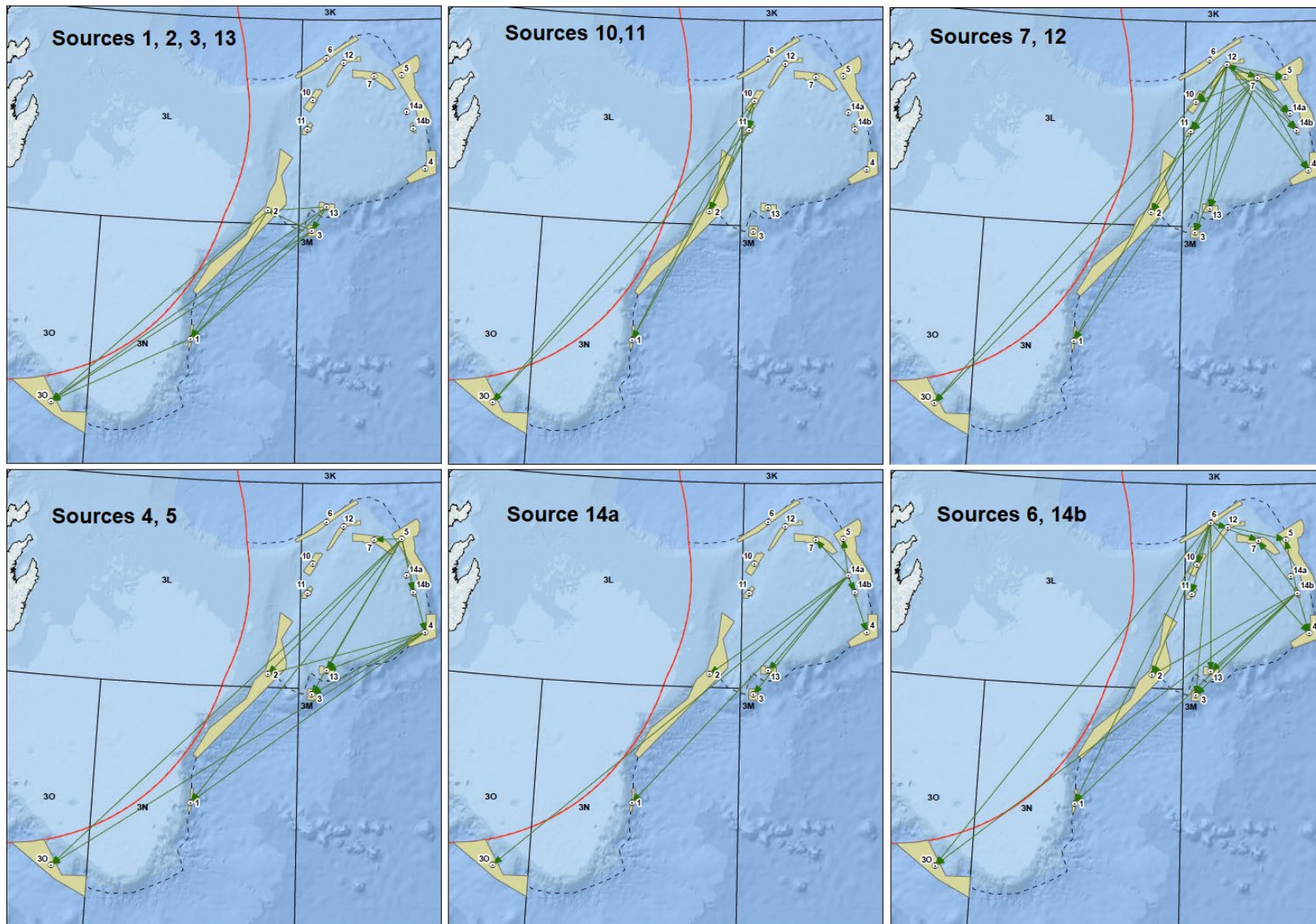
Figure 27. Unidirectional (source to sink) connectivity for the NAFO Closed Areas in the NAFO Regulatory Area (numbered as in Figure 24) which showed connectivity (Figure 26). Each panel shows connections for different source areas to avoid congestion.

Table 26. Nearest neighbour distances (km) calculated from centroid to centroid for the closed areas in the NAFO Regulatory Area (numbered as in Figure 24) with connections not found in the Lagrangian Particle Tracking (LPT) simulations removed. The mean nearest-neighbour distance for each closed area, as a measure of relative isolation, is shown below the rows. Closed areas are numbered according to the NAFO Conservation and Enforcement Measures. All calculations were performed using NAD83 UTM 23 projection.*Area 6 is the upstream closure so no other areas can connect with it. Similarly 3O is the downstream closure so it can't connect with any other areas.

Area No.	Description	Polygon Area km²	Area 1	Area 2	Area 3	Area 4	Area 5	Area 6*	Area 7	Area 10	Area 11	Area 12	Area 13	Area 14a	Area 14b	3O*
								Source Particle Release Areas								
Area 1	Tail of the Bank	172	---	263	286	510	594	549	564	472	423	555	333	551	539	269
Area 2	Flemish Pass	5,771		---	85	287	335	288	302	210	160	292	104	300	294	
Area 3	Beothuk Knoll	308			---	228	316	305	294			301	49	268	254	
Area 4	E Flemish Cap	1,358				---	169	261	186			234		105	74	
Area 5	NE Flemish Cap	2,879					---	136	48			104		65	95	
Area 6	Sackville Spur	987						---								
Area 7	N Flemish Cap	1,053					48	90	---			58		85	114	
Area 10	NW Flemish Cap	527						78	116	---		85				
Area 11	NW Flemish Cap	220						130	150	52	---	132				
Area 12	NW Flemish Cap	511						32	58			---				
Area 13	Beothuk Knoll	338				186	267	262	245			255	---	219	206	
Area 14a	NE Flemish Cap	50							85			140		---		
Area 14b	NE Flemish Cap	104					95		114			167		31	---	
3O	3O Coral Closure	3,694	269	508	548	775	842	774	807	702	658	787	593	806	798	---
Mean Nearest-Neighbour Distance (Centroid-Centroid)			269	264	257	267	256	252	235	221	215	242	235	237	241	269

(Left vertical label: **Sink Closed Areas**)

Table 27. Nearest neighbour distances (km) calculated from the nearest edges for the closed areas in the NAFO Regulatory Area (numbered as in Figure 24) with connections not found in the Lagrangian Particle Tracking (LPT) simulations removed. The mean nearest-neighbour distance for each closed area, as a measure of relative isolation, is shown below the rows. Closed areas are numbered according to the NAFO Conservation and Enforcement Measures. All calculations were performed using NAD83 UTM 23 projection.

	Area No.	Description	Polygon Area km²	Source Particle Release Areas													
				Area 1	Area 2	Area 3	Area 4	Area 5	Area 6	Area 7	Area 10	Area 11	Area 12	Area 13	Area 14a	Area 14b	3O
Sink Closed Areas	Area 1	Tail of the Bank	172	---	55	254	454	532	470	518	427	386	480	299	525	514	211
	Area 2	Flemish Pass	5,771		---	52	202	230	127	176	83	43	137	58	212	214	
	Area 3	Beothuk Knoll	308			---	178	254	259	268			244	27	250	236	
	Area 4	E Flemish Cap	1,358				---	48	229	122			195		72	36	
	Area 5	NE Flemish Cap	2,879					---	80	11			57		12	10	
	Area 6	Sackville Spur	987						---								
	Area 7	N Flemish Cap	1,053					11	40	---			15		40	67	
	Area 10	NW Flemish Cap	527						32	58	---		11				
	Area 11	NW Flemish Cap	220						81	108	18	---	69				
	Area 12	NW Flemish Cap	511						16	15			---				
	Area 13	Beothuk Knoll	338				133	205	221	223			202	---	200	186	
	Area 14a	NE Flemish Cap	50							40			114		---		
	Area 14b	NE Flemish Cap	104					10		67			141		17	---	
	3O	3O Coral Closure	3,694	211	284	497	697	775	686	753	657	619	712	542	768	757	---
	Mean Nearest-Neighbour Distance (Edge-Edge)			211	170	268	333	258	204	197	296	349	198	232	233	253	211

Table 28. Revised Isolation/Proximity indices for the VME closures in the NAFO Regulatory Area after removal of unlikely connection links.

Distance Measurement Method	Mean Nearest-Neighbour Distance Over All Polygons Pairs	Proximity Index (PX)
Centroid-Centroid	247	
Edge-Edge	244	190.24

Conclusions

The results of our analyses are presented in Tables 29 and 30 in comparison with those completed last year (NAFO, 2020). In both the case of the VME polygons and the new closed areas that will come into effect in 2022, there was a decrease in the mean nearest-neighbour distance over all polygons calculated centroid to centroid when only connections confirmed through the LPT simulations were considered. This is a straightforward recalculation and has nothing to do with fragmentation. However, the comparison of the current (NAFO, 2020) and the new closures (Table 29) showed little change in the mean nearest-neighbour distance over all polygons but shows a large increase in PX. This indicates that PX is sensitive to the change in configuration within the spatial extent. The new closures have fewer larger closures on Flemish Cap and the result is picked up by PX. As a result, we expect PX to respond to changes in the configuration of the VME polygons which we plan to simulate in the next phase of this work. All closed areas show retention and 46% of the possible connections were considered viable.

Table 29. Summary of Isolation/Proximity Indices for large-sized sponge VMEs and the NAFO Closed Areas with and without removal of unlikely connections established by Lagrangian particle tracking analyses.

Isolation/Proximity Index	2020 Closures (NAFO, 2020)	New 2022 Closures All Connections	New 2022 Closures Likely Connections Only
Mean Nearest-Neighbour Distance Over All Polygons Pairs Centroid-Centroid	282	290	247
Mean Nearest-Neighbour Distance Over All Polygons Pairs Edge-Edge	236	236	244
Proximity Index (PX)	452.00	782.96	660.60

The percentage of connected VME polygons (excluding retention) is low among all the VME Indicator taxa and ranged from 11% for the black coral and bryozoans to 36% for the sea pens. The percentage of retention among the VME polygons was very high for most and ranged from 89% for the sponges to 11% for the sea squirts. These percentages relate to the spatial configuration of the VME polygons with respect to the prevailing bottom currents. They are considered to be maximal estimates in most cases as for some groups such as the sponges, byrozoans, sea squirts and black corals, the larvae may only disperse in the water column for a few hours if at all. The percentages of connections and retentions (Table 30) among the VME may represent natural dispersal patterns required for maintenance of the VMEs, assuming that these VME have not been already modified by bottom fishing. If so then the high % retention in these areas (50% or more for all but bryozoans and sea squirts) may be a factor in maintaining the high biomass areas and for creating their spatial distinctiveness allowing the kernel density analysis to perform as it does.

The new results (Table 30) for the isolation/proximity indices for the VME polygons differ only because of the removal of some connections. All values decreased with removal of connections except for sea squirt (*Boltenia ovifera*) average centroid to centroid distances which increased slightly. These values and connections should form the baseline for monitoring future changes and for undergoing simulations.

Table 30. Summary of Isolation/Proximity Indices for all of the VMEs with (from NAFO, 2020) and without (revised herein) removal of unlikely connections established by Lagrangian particle tracking analyses.

Isolation/ Proximity Index	Sponge VME (NAFO, 2020)	Sponge VME Revised	Sea Pen VME (NAFO, 2020)	Sea Pen VME Revised	LGC VME (NAFO, 2020)	LGC VME Revised	SGC VME (NAFO, 2020)	SGC VME Revised	Black Coral VME (NAFO, 2020)	Black Coral Revised	Sea Squirt VME (NAFO, 2020)	Sea Squirt Revised	Bryozoan VME (NAFO, 2020)	Bryozoan VME Revised
Mean Nearest-Neighbour Distance Over All Polygons Pairs Centroid-Centroid	271	161	363	303	320	299	311	307	289	80	212	214	175	61
Mean Nearest-Neighbour Distance Over All Polygons Pairs Edge-Edge	190	70	333	263	299	269	292	285	272	48	199	194	166	34
Proximity Index (PX)	1111.80	806.04	394.2	385.0	255.1	180.6	125.2	25.3	108.9	106.2	801.5	682.9	717.1	699.5
% Connection		22		36		15		33		11		26		11
% Retention		89		73		58		67		50		11		35

References

Armsworthy, S., MacDonald, B.A., and Ward, J.E. (2001). Feeding activity, absorption efficiency and suspension feeding processes in the ascidian, *Halocynthia pyriformis* (Stolidobranchia: Ascidiacea): responses to variations in diet quantity and quality. J. Exp. Mar. Biol. Ecol. 260, 41-69.

Avant, P. (2004). *Eucratea loricata* An encrusting bryozoan. In Tyler-Walters H. and Hiscock K. Marine Life Information Network: Biology and Sensitivity Key Information Reviews, [on-line]. Plymouth: Marine Biological Association of the United Kingdom. [cited 22-11-2021]. Available from: https://www.marlin.ac.uk/species/detail/1751

Bracco A., Liu, G., Galaska, M., Quattrini, A. M., and Herrera, S. (2019). Integrating physical circulation models and genetic approaches to investigate population connectivity in deep-sea corals. J. Mar. Syst. 198, 103189. doi: 10.1016/j.jmarsys.2019.103189

Delandmeter, P., and van Sebille, E. (2019). The Parcels v2.0 Lagrangian framework: new field interpolation schemes. Geosci. Model Devel. 12, 3571–3584.

Goldsmit, J., Nudds, S. H., Stewart, D. B., Higdon, J. W., Hannah, C. G., and Howland, K. L. (2019). Where else? Assessing zones of alternate ballast water exchange in the Canadian eastern Arctic. Mar. Poll. Bull. 139, 74-90.

Gustafson, E.J., and Parker, G.R. (1994). Using an index of habitat patch proximity for landscape design. Landsc. Urban Plan. 29, 117-130.

Haddad, N.M., Brudvig, L.A., Clobert, J., Davies, K.F., Gonzalez, A., Holt, R.D., Lovejoy, T.E., Sexton, J.O., Austin, M.P., Collins, C.D., Cook, W.M., Damschen, E.I., Ewers, R.M., Foster, B.L., Jenkins, C.N., King, A.J., Laurance, W.F., Levey, D.J., Margules, C.R., Melbourne, B.A., Nicholls, A.O., Orrock, J.L., Song, D.-Z., and Townshend, J.R. (2015). Habitat fragmentation and its lasting impact on Earth's ecosystems. Science Advances 20 Mar 2015: Vol. 1, no. 2, e1500052 DOI: 10.1126/sciadv.1500052.

Kenchington, E., Wang, Z., Lirette, C., Murillo, J. F., Guijarro, J., Yashayaev, I., et al. (2019). Connectivity modelling of areas closed to protect vulnerable marine ecosystems in the northwest Atlantic. Deep-Sea Res. I 143, 85–103.

Kenchington, E., Murillo, F.J., Lirette, C., Sacau, M., Koen-Alonso, M., Kenny, A., Ollerhead, N., Wareham, V., and Beazley, L. (2014). Kernel density surface modelling as a means to identify significant concentrations of vulnerable marine ecosystem indicators. PLoS ONE 9(10): e109365.

Keough, M. J. (1989) Dispersal of the bryozoan *Bugula neritina* and effects of adults on newly metamorphosed juveniles. Mar. Ecol. Prog. Ser. 57, 163-171.

Kim, G. J. (2020). Embryonic development and metamorphosis of the ascidian *Halocynthia aurantium*. JMLS 5, 58-63. https://www.koreascience.or.kr/article/JAKO202023162045712.pdf

Lacalli, T. (1980). Annual spawning cycles and planktonic larvae of benthic invertebrates from Passamaquoddy Bay, New Brunswick. Can. J. Zool. 59, 433-440.

Lange, M., and van Sebille, E. (2017). Parcels v0.9: prototyping a Lagrangian Ocean Analysis framework for the petascale age. Geosci. Model Devel. 10, 4175-4186.

Ma, K.C.K., Deibel, D., Law, K.K.M., Aoki, M., McKenzie, C.H., and Palomares, M.L.D. (2017). Richness and zoogeography of ascidians (Tunicata: Ascidiacea) in eastern Canada. Can. J. Zool. 95, 51-59.

Miller, K.J. (1998). Short-distance dispersal of black coral larvae: inference from spatial analysis of colony genotypes. MEPS 163, 225-233.

Miller, K.J. (1996) Piecing together the reproductive habits of New Zealand's endemic black corals. Water Atmos. 4, 18-19.

Murillo, F. J., Serrano, A., Kenchington, E., and Mora, J. (2016). Epibenthic assemblages of the Tail of the Grand Bank and Flemish Cap (northwest Atlantic) in relation to environmental parameters and trawling intensity. Deep Sea Res. Part I Oceanogr. Res. Pap. 109, 99–122.

NAFO. (2021). Northwest Atlantic Fisheries Organization Conservation and Enforcement Measures 2021. NAFO/COM Doc. 21-01.

NAFO. (2020). Report of the Scientific Council Working Group on Ecosystem Science and Assessment, 17 - 26 November 2020, Dartmouth, Nova Scotia, Canada. NAFO SCS Doc. 19/23.

Powell, N.A. (1968) Bryozoa (Polyzoa) of Arctic Canada. J. Fish. Res. Bd. Canada 25, 2269-2320.

Ryland, J.S. (1974). Behaviour, settlement and metamorphosis of bryozoan larvae: a review. Thalassia Jugoslavica 10, 239-262.

Tischendorf, L., and Fahrig, L. (2000). On the usage and measurement of landscapeconnectivity. Oikos 90, 7–19.

Wagner, D., Waller, R.G., and Toonen, R.J. (2011). Sexual reproduction of Hawaiian black corals, with a review of the reproduction of antipatharians (Cnidaria: Anthozoa: Hexacorallia). Invert. Biol., 30, 211-225.

Wang, S., Kenchington, E., Wang, Z., and Davies, A.J. (2021). Life in the fast lane: Modeling the fate of glass sponge larvae in the Gulf Stream. Front. Mar. Sci. 8:701218. doi: 10.3389/fmars.2021.701218

Wang, S., Kenchington, E.L., Wang, Z., Yashayaev I., and Davies, A.J. (2020). 3-D Ocean particle tracking modeling reveals extensive vertical movement and downstream interdependence of closed areas in the northwest Atlantic. Sci. Rep. 10, 21421. doi: 10.1038/s41598-020-76617-x

Wang, Z., Brickman, D., and Greenan, B.J.W. (2019). Characteristic evolution of the Atlantic Meridional Overturning Circulation from 1990 to 2015: An eddy-resolving ocean model study. Deep Sea Res. I 149, 103056. doi: 10.1016/j.dsr.2019.06.002

Wang, Z., Lu, Y., Greenan, B., and Brickman, D. (2018). BNAM: An eddy-resolving North Atlantic Ocean model to support ocean monitoring. Can. Tech. Rep. Hydrogr. Ocean Sci. 327: vii + 18p.

Wilson, M.C., Chen, X.-Y., Corlett, R.T., Didham, R.K., Ding, P., Holt, R.D., Holyoak, M., Hu, G., Hughes, A.C., Jiang, L., Laurance, W.F., Liu, J., Pimm, S.L., Robinson, S.K., Russo, S.E., Si, X., Wilcove, D.S., Wu, J., and Yu, M. (2016). Habitat fragmentation and biodiversity conservation: key findings and future challenges. Landscape Ecology 31, 219–227.

Xu, G., McGillicuddy, D. J., Jr., Mills, S. W., and Mullineaux, L. S. (2018). Dispersal of hydrothermal vent larvae at East Pacific Rise 9–10°N segment. J. Geophys. Res. Oceans 123, 7877–7895.

Zeng, X., Adams, A., Roffer, M., and He, R. (2019). Potential connectivity among spatially distinct management zones for bonefish (*Albula vulpes*) via larval dispersal. Environ. Biol. Fish. 102, 233–252.